The Plant Cell, Vol. 23: 3824–3841, October 2011, www.plantcell.org

Arabidopsis Sigma Factor Binding Proteins Are Activators of the WRKY33 Transcription Factor in Plant Defense [W]

Zhibing Lai,[a] Ying Li,[a,1] Fei Wang,[a] Yuan Cheng,[a,b] Baofang Fan,[a] Jing-Quan Yu,[b] and Zhixiang Chen[a,b,2]

[a] Department of Botany and Plant Pathology, Purdue University, West Lafayette, Indiana 47907-2054
[b] Department of Horticulture, Zhejiang University, Hangzhou 310058, China

Necrotrophic pathogens are important plant pathogens that cause many devastating plant diseases. Despite their impact, our understanding of the plant defense response to necrotrophic pathogens is limited. The WRKY33 transcription factor is important for plant resistance to necrotrophic pathogens; therefore, elucidation of its functions will enhance our understanding of plant immunity to necrotrophic pathogens. Here, we report the identification of two WRKY33-interacting proteins, nuclear-encoded SIGMA FACTOR BINDING PROTEIN1 (SIB1) and SIB2, which also interact with plastid-encoded plastid RNA polymerase SIGMA FACTOR1. Both SIB1 and SIB2 contain an N-terminal chloroplast targeting signal and a putative nuclear localization signal, suggesting that they are dual targeted. Bimolecular fluorescence complementation indicates that WRKY33 interacts with SIBs in the nucleus of plant cells. Both SIB1 and SIB2 contain a short VQ motif that is important for interaction with WRKY33. The two VQ motif–containing proteins recognize the C-terminal WRKY domain and stimulate the DNA binding activity of WRKY33. Like *WRKY33*, both *SIB1* and *SIB2* are rapidly and strongly induced by the necrotrophic pathogen *Botrytis cinerea*. Resistance to *B. cinerea* is compromised in the *sib1* and *sib2* mutants but enhanced in *SIB1*-overexpressing transgenic plants. These results suggest that dual-targeted SIB1 and SIB2 function as activators of WRKY33 in plant defense against necrotrophic pathogens.

INTRODUCTION

Plants have an innate immunity system for detecting and mounting defense responses to invading microbial pathogens. The majority of research on plant innate immunity has focused on biotrophic or hemibiotrophic pathogens, which parasitize living plant tissues during all or part of their life cycles. The plant innate immune system against biotrophic pathogens consists of two interconnected branches, pathogen-associated molecular pattern–triggered immunity (PTI) and effector-triggered immunity (ETI) (Jones and Dangl, 2006). PTI is activated by receptor-mediated recognition of pathogen-associated molecular patterns, such as bacterial flagellin, through a mitogen-activated protein kinase signaling cascade. Pathogens can deliver effector proteins to plant cells to suppress PTI and promote pathogen virulence. Through coevolution, some effectors are recognized by plant resistance (R) proteins and activate strong ETI (Jones and Dangl, 2006). ETI involves a complex defense program, including the production of reactive oxygen species (ROS) and salicylic acid (SA) and the hypersensitive response (Jones and Dangl, 2006).

Less is known about plant defense against necrotrophic pathogens, which kill host cells before colonizing them. Gene-for-gene resistance to necrotrophs is rare, and *R* gene–mediated hypersensitive cell death actually facilitates infection by necrotrophic pathogens (Govrin and Levine, 2000). Molecular and genetic studies have identified several genes, including *Arabidopsis thaliana MITOGEN-ACTIVATED PROTEIN KINASE4* (*MPK4*) (Brodersen et al., 2006), *SUPPRESSOR OF SA INSENSITIVITY2* (encoding a stearoyl-ACP desaturase) (Nandi et al., 2005), *BOTRYTIS SUSCEPTIBLE1* (encoding an R2R3MYB transcription factor) (Mengiste et al., 2003b), and *BOTRYTIS-INDUCED KINASE1* (encoding a receptor-like protein kinase) (Veronese et al., 2006), involved in plant resistance to necrotrophic pathogens. The mutants for these genes exhibit growth abnormality with high SA levels, and their susceptibility to necrotrophic pathogens is associated with resistance to biotrophic pathogens and is dependent on *ENHANCED DISEASE SUSCEPTIBILITY1* (*EDS1*), *PHYTOALEXIN DEFICIENT4* (*PAD4*), and *EDS5*, which regulate SA biosynthesis (Nandi et al., 2005; Brodersen et al., 2006; Veronese et al., 2006). Therefore, their roles in resistance to necrotrophic pathogens may be indirect. In *Arabidopsis*, the jasmonate (JA)-insensitive *coi1* and ethylene-insensitive *ein2* mutants are compromised in resistance to the necrotrophic fungal pathogen *Botrytis cinerea* (Penninckx et al., 1996, 1998; Thomma et al., 1998). Accumulation of camalexin in *Arabidopsis*, a phytoalexin, is correlated with resistance to necrotrophic pathogens, and mutants deficient in camalexin are compromised in resistance to necrotrophic pathogens (Thomma et al., 1999; Ferrari et al., 2003). However, susceptibility to necrotrophic pathogens with normal accumulation of JA-regulated *PDF1.2* expression and camalexin has been

[1] Current address: Department of Horticulture, Nanjing Agricultural University, Nanjing, China 210095.
[2] Address correspondence to zhixiang@purdue.edu.
The author responsible for distribution of materials integral to the findings presented in this article in accordance with the policy described in the Instructions for Authors (www.plantcell.org) is: Zhixiang Chen (zhixiang@purdue.edu).
[W] Online version contains Web-only data.
www.plantcell.org/cgi/doi/10.1105/tpc.111.090571

documented (Ferrari et al., 2003; Mengiste et al., 2003a; Veronese et al., 2004), suggesting that other unknown defense pathways may be equally or even more important. Overall, our understanding of plant defense against necrotrophic pathogens is limited.

We have previously shown that in *Arabidopsis*, WRKY33, a member of the WRKY transcription factor superfamily characterized by the hallmark heptapeptide WRKYGQK and a novel zinc-finger motif, is important for plant resistance to necrotrophic pathogens (Zheng et al., 2006). T-DNA insertion mutants for *WRKY33* are highly susceptible to necrotrophic pathogens *B. cinerea* and *Alternaria brassicicola*, while overexpression of *WRKY33* enhances resistance to the necrotrophic pathogens (Zheng et al., 2006). Although it has been reported that the *wrky33-2* T-DNA insertion mutant contained significantly more transcripts of SA-regulated *PR1* prior to or following infection with the bacterial pathogen *Pseudomonas syringae* pv tomato DC3000 (Andreasson et al., 2005), we found that the mutant as well as another independent T-DNA insertion mutant (*wrky33-1*) supported normal growth of the bacterial pathogen (Zheng et al., 2006). However, overexpression of *WRKY33* resulted in enhanced susceptibility to the bacterial pathogen (Zheng et al., 2006). These results suggest that WRKY33 has an important and rather specific role in plant resistance to necrotrophic pathogens (Zheng et al., 2006), although it might also be involved in some aspects of plant responses to other types of microbial pathogens.

Arabidopsis WRKY33 and closely related WRKY25 interact with MAP KINASE SUBSTATE1 (MKS1), a VQ motif–containing protein substrate of *Arabidopsis* MPK4 (Andreasson et al., 2005). It has been shown that in the absence of pathogen infection, MPK4 exists in nuclear complexes with WRKY33 through mutual interactions with MKS1 (Qiu et al., 2008). Upon *Pseudomonas* infection or flagellin treatment, activated MPK4 phosphorylates MKS1 and releases WRKY33, which then targets the expression of *PAD3*, which encodes a biosynthetic enzyme for the phytoalexin camalexin (Qiu et al., 2008). Since this MPK4-releasing-WRKY33 model is based on studies using *Pseudomonas* infection and flagellin treatment, it may not necessarily be applicable to how WRKY33 is regulated during plant responses to necrotrophic pathogens. Indeed, unlike WRKY33, which plays an important role in plant resistance to necrotrophic pathogens, MKS1 affects only SA-dependent defense (Andreasson et al., 2005; Petersen et al., 2010). In addition, as will be described below, unlike in *Pseudomonas*-infected or flagellin-treated plants (Qiu et al., 2008), induced transcript levels of *PAD3* were almost as high in a *wrky33* mutant as in wild-type plants 24 h after *B. cinerea* infection. Therefore, the regulation of WRKY33 in plant defense against necrotrophic pathogens may be more complicated than or different from the regulation described in the simple MPK4-releasing-WRKY33 model.

Here, we report the identification and functional analysis of two WRKY33-interacting proteins in WRKY33-mediated plant defense against necrotrophic pathogens. Using the yeast two-hybrid system, we have discovered that WRKY33 binds in the nucleus two closely related VQ motif–containing proteins, SIB1 and SIB2, which also interact with the plastid-encoded plastid RNA polymerase σ-factor SIG1 (Morikawa et al., 2002). Like *WRKY33*, both *SIB1* and *SIB2* are rapidly and strongly induced by necrotrophic pathogens. The two dual-targeted SIB proteins recognize the C-terminal WRKY domain of WRKY33 and stimulate the DNA binding activity of WRKY33. Mutations of *SIB1* and *SIB2* compromise while *SIB1* overexpression enhances plant resistance to the necrotrophic pathogen *B. cinerea*. These results suggest that dually targeted SIB proteins function as activators of the WRKY33 transcription factor and positively regulate plant defense against necrotrophic pathogens. The discovery of VQ motif–containing proteins capable of recognizing the WRKY domain and stimulating the DNA binding activity of WRKY33 will further our understanding of how plant WRKY proteins regulate diverse plant biological processes.

RESULTS

Role of WRKY33 in *B. cinerea*–Induced *PAD3* Expression

One critical line of evidence supporting the MPK4-releasing-WRKY33 model for regulation of WRKY33 during plant defense is the observation that WRKY33 is required for induced expression of *PAD3* upon *Pseudomonas* infection or flagellin treatment (Qiu et al., 2008). Recently, it was reported that the *wrky33* mutant seedlings grown in liquid culture medium were severely compromised in *Botrytis*-induced *PAD3* expression (Mao et al., 2011). In this study, we analyzed the role of WRKY33 in *Botrytis*-induced *PAD3* expression in soil-grown mature plants, which are typically used for evaluation of plant responses to the necrotrophic pathogen. We sprayed both *Arabidopsis* wild-type and *wrky33* mutant plants with a buffer (mock inoculation) or *B. cinerea*, and total RNA was isolated from inoculated leaves for detection of *PAD3* transcripts using RNA gel blotting. As shown in Figure 1, the level of *PAD3* transcripts was low in uninoculated or mock-inoculated wild-type and *wrky33* mutant

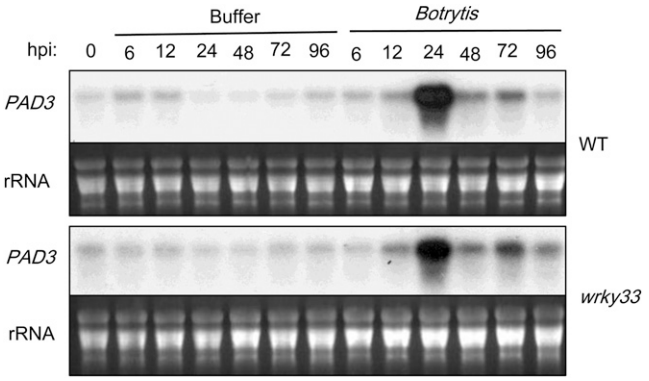

Figure 1. Expression of *PAD3* in Response to *B. cinerea*.

Wild-type (WT) and *wrky33* mutant plants were inoculated with *B. cinerea* as described in Methods. The inoculated leaves were collected at the indicated hours after inoculation (hpi) for RNA isolation. RNA gel blot analysis was performed with a ^{32}P-labeled *PAD3*. Ethidium bromide staining of rRNA is shown for the assessment of equal loading. The experiments were repeated twice with similar results.

leaves. *PAD3* transcripts were also low at 6 and 12 h after inoculation (HAI) with *B. cinerea* in wild-type and *wrky33* mutant leaves. At 24 HAI, however, we observed a drastic increase in *PAD3* transcript levels in the wild-type plants (Figure 1). In the *wrky33* mutant plants, we also observed a great increase in the transcript level for *PAD3* at 24 HAI, although the increase was somewhat smaller than in wild-type plants (Figure 1). The strong induction of *PAD3* in both *B. cinerea*–inoculated wild-type and *wrky33* plants appeared to be transient as its transcript levels declined greatly by 48 to 96 HAI (Figure 1). Overall, we observed no drastic difference between soil-grown wild-type and *wrky33* mutant plants in the changes in *PAD3* transcript levels after *B. cinerea* infection.

The MPK4-releasing-WRKY33 model has been proposed based mostly on the dynamic changes of the MPK4-MSK1-WRKY33 complexes in the nucleus and the opposite roles of MPK4 and WRKY33 in the regulation of *PAD3* expression upon *Pseudomonas* infection or flagellin treatment (Qiu et al., 2008). The observation that *B. cinerea*–induced *PAD3* expression was not greatly compromised in soil-grown mature *wrky33* mutant suggests differential roles and regulation of WRKY33 in plant responses to different types of microbial pathogens. In light of the difference in *PAD3* induction between young seedlings grown in liquid medium and soil-grown mature plants, it also appears that the role of WRKY33 in *Botrytis*-induced *PAD3* expression is strongly affected by the age and growth conditions of plants. In addition, unlike WRKY33, which plays an important role in plant defense against necrotrophic pathogens, the previously identified WRKY33-interacting MKS1 affects only SA-dependent defense (Andreasson et al., 2005). These observations prompted us to explore other WRKY33-interacting proteins that may be involved in WRKY33-mediated defense against necrotrophic pathogens.

Identification of SIB1 and SIB2 as WRKY33-Interacting Proteins

WRKY33, consisting of 519 amino acid residues, is a group I WRKY protein with two WRKY domains. To identify WRKY33-interacting proteins using a Gal4 transcription activation-based yeast two-hybrid system, we first fused whole WRKY33 protein with the DNA binding domain (BD) of Gal4 (BD-W33) but found that the fusion protein itself has transcription-activating activity and activated reporter genes in yeast cells. We then fused Gal4 BD with the C-terminal two-thirds of WRKY33 starting from amino acid residue 181 (BD-W33Δ1) and found little activation of reporter genes when the fusion protein was expressed in yeast cells. Using BD-W33Δ1 as bait, we screened 3×10^6 independent transformants of an *Arabidopsis* cDNA prey library. Twenty-three clones encoding SIGMA FACTOR BINDING PROTEIN1 (SIB1) (Figure 2A) were identified by prototrophy for His and by *LacZ* reporter gene expression through assays of β-galactosidase activity.

SIB1 is a nuclear-encoded protein of 151 amino acid residues and interacts with the plastid-encoded plastid RNA polymerase σ-factor SIG1 in both yeast two-hybrid and pull-down assays (Morikawa et al., 2002). Consistent with their interaction with plastid-localized SIG1, SIB1 contains an N-terminal chloroplast localization signal peptide and is transported into chloroplasts when fused with green fluorescent protein (GFP) (Morikawa et al., 2002). Therefore, it is intriguing that SIB1 was identified as an interacting partner of WRKY33, which is localized to the nucleus (Zheng et al., 2006). However, in addition to the N-terminal chloroplast localization signal peptide, SIB1 contains a putative nuclear localization signal (NLS) (Figure 2A) and therefore may be dual targeted. To test this and confirm its interaction with WRKY33, we examined the interaction in plant cells using bimolecular fluorescence complementation (BiFC) in *Agrobacterium tumefaciens*–infiltrated tobacco (*Nicotiana benthamiana*) leaves (Cui et al., 2007). We fused WRKY33 to the N-terminal yellow fluorescent protein (YFP) fragment (WRKY33-N-YFP) and SIB1 to the C-terminal YFP fragment (SIB1-C-YFP). When fused WRKY33-N-YFP was coexpressed with SIB1-C-YFP in tobacco leaves, BiFC signal was detected in the nuclear compartment of transformed cells, based on staining with 4′,6-diamidino-2-phenylindole (DAPI) (Figure 2B). Control experiments in which WRKY33-N-YFP was coexpressed with unfused C-YFP or unfused N-YFP was coexpressed with SIB1-C-YFP did not show any fluorescence. Furthermore, when WRKY48-N-YFP or WRKY18-N-YFP was coexpressed with SIB1-C-YFP, we observed no fluorescence (Figure 2B; see Supplemental Figure 1A online). These experiments indicate that WRKY33 interacts with SIB1 in the nuclear compartment of plant cells.

To confirm their interaction in plant cells, we performed coimmunoprecipitation. We previously generated transgenic *wrky33-2* mutant plants harboring a *WRKY33-TAP* (tandem affinity purification) fusion construct under the control of the native promoter (Lai et al., 2011). Immunoblotting detected inducible expression of the transgene and *WRKY33-TAP* can fully complement the *wrky33* mutant for resistance to *B. cinerea* (Lai et al., 2011). The transgenic plants were infiltrated with agrobacterial cells containing the *SIB1-4xmyc* tag construct under the cauliflower mosaic virus (*CaMV*) *35S* promoter. We also infiltrated the transgenic *WRKY33-TAP* plants with agrobacterial cells containing a mutant SIB1 tag construct (*SIB1/NLSmut-4xmyc*), in which the nucleotides for the basic amino acid residues of SIB1 NLS were mutated to those for Ala residues. Total proteins from infiltrated plants were subjected to tandem affinity purification as we previously described for EDS1 and PAD4 (Xing and Chen, 2006). The eluted proteins from the purification procedure were analyzed by immunoblotting using the anti-myc tag antibody. The protein complexes purified from transgenic WRKY33-TAP plants infiltrated with *SIB1-4xmyc*–containing agrobacteria generated positive interactions with the anti-myc antibody (Figure 2C). By contrast, proteins purified from nontransgenic plants infiltrated with *SIB1-4xmyc*–containing agrobacteria generated no interaction to the anti-myc antibody (Figure 2C). Likewise, protein complexes purified from transgenic WRKY33-TAP plants infiltrated with the *SIB1/NLSmut-4xmyc*–containing agrobacteria generated no cross-reactivity to the antibody (Figure 2C). The coimmunoprecipitation supported interaction of WRKY33 with SIB1 in the nucleus of plant cells.

Chloroplast import of SIB1 has been previously demonstrated by the transient expression of the SIB1-GFP fusion protein in the protoplasts, but no effort was made to analyze a possible SIB1-GFP

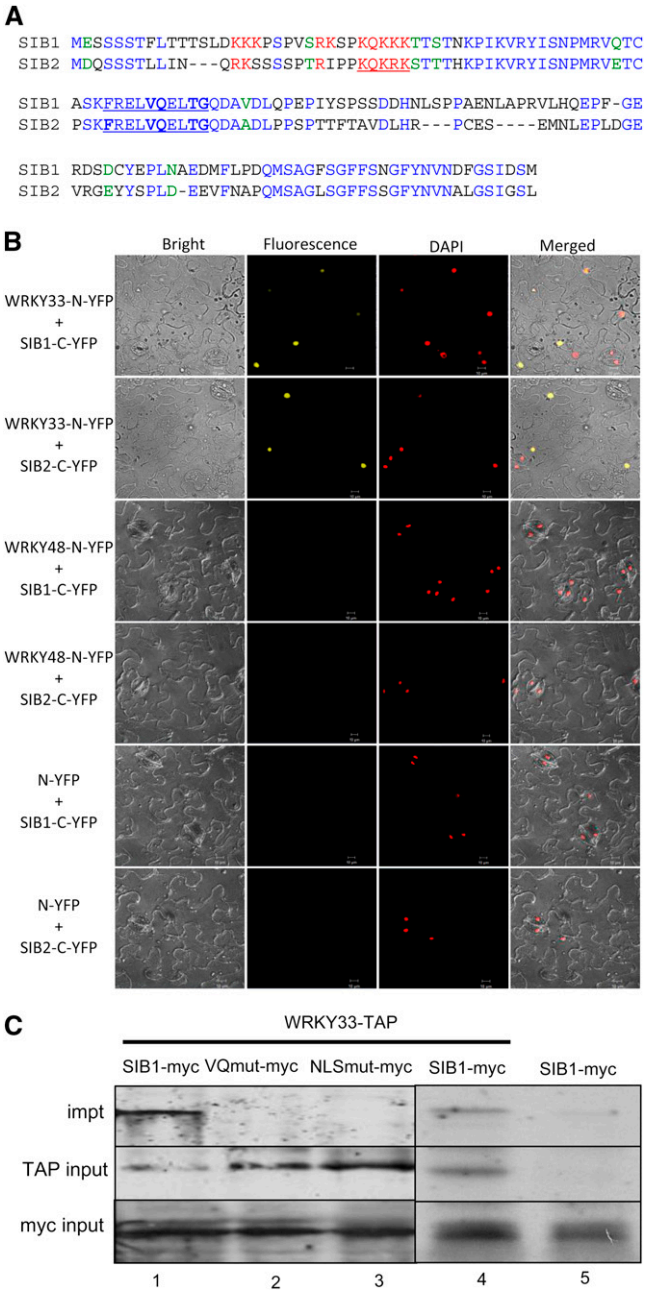

Figure 2. Interactions of WRKY33 with SIB1 and SIB2.

(A) Sequence comparison of SIB1 and SIB2. Amino acids identical in two proteins are blue, and residues similar in two proteins are green. The Arg (R) and Lys (K) residues in the putative NLSs are red. The highly conserved FXXXVQXXTG (X, any amino acid) sequences are underlined.
(B) BiFC analysis of WRKY33 interactions in planta with SIB1 and SIB2 proteins. Fluorescence was observed in the nuclear compartment of *N. benthamiana* leaf epidermal cells, which results from complementation of the N-terminal part of the YFP fused with WRKY33 (WRKY33-N-YFP) or with the C-terminal part of the YFP fused with SIB1 (SIB1-C-YFP) or SIB2 (SIB2-C-YFP). No fluorescence was observed when WRKY48-N-YFP was coexpressed with SIB1-C-YFP. Bright-field images, YFP epifluorescence images, DAPI staining, and overlay images of the same cells are shown.

signal in the nucleus (Morikawa et al., 2002). To further investigate the subcellular localization of *Arabidopsis* SIB1, we generated transgenic *Arabidopsis* plants expressing a SIB1-GFP fusion under the control of the *CaMV 35S* promoter. In these transgenic plants, we observed a SIB1-GFP signal in chloroplasts, as expected (see Supplemental Figure 1B online). Significantly, we also observed GFP fluorescent signal in the nuclear compartment based on DAPI staining (see Supplemental Figure 1B online). Thus, *Arabidopsis* SIB1 is localized in both chloroplasts and the nucleus.

SIB1 has close structural homology to SIB2 (Figure 2A), which also interacts with the plastid-localized SIG1 (Morikawa et al., 2002). Like SIB1, SIB2 contains not only an N-terminal chloroplast targeting signal peptide but also a putative NLS (Figure 2A) and therefore may also be dual targeted. To determine whether WRKY33 also interacts with SIB2, we first used yeast two-hybrid assays and confirmed their interaction by prototrophy for His and by *LacZ* reporter gene expression through assays of β-galactosidase activity. We also fused SIB2 to the C-terminal YFP fragment (SIB2-C-YFP) and coexpressed it with WRKY33-N-YFP in tobacco. Indeed, we observed a BiFC signal in the nuclear compartment of transformed cells, based on staining with DAPI (Figure 2B). Thus, both SIB1 and SIB2 are interacting partners of WRKY33.

Importance of the VQ Motif of SIB1 for Interaction with WRKY33

WRKY33 also interacts with MKS1, a substrate of MPK4 from *Arabidopsis* (Andreasson et al., 2005). MKS1, SIB1, and SIB2 all belong to a novel family of plant proteins that contain a conserved FXXXVQXXTG motif (X, any amino acid) (Figure 2A). Other than the short VQ motif, MKS1 and SIBs share little sequence homology. Yeast two-hybrid assays have shown that the domain containing the VQ motif in MKS1 is required for its interaction with WRKY33 (Andreasson et al., 2005). To determine whether the short VQ motif of SIB1 is also required for its interaction with WRKY33, we generated a mutant SIB1 (SIB1$^{V62A/Q63A}$) in which the conserved Val (V) and Gln (Q) residues in the VQ motif were replaced by Ala (A) residues. To monitor levels of expressed proteins in yeast cells during the yeast two-hybrid assays, we inserted a myc and FLAG tag behind the binding and activation domains of the pBD-GAL4 bait and pAD-GaL4 prey vectors, respectively. The mutant SIB1$^{V62A/Q63A}$ (VQmut) was then fused with the AD-FLAG domain of Gal4 in the modified prey vector and cotransformed with the myc-WRKY33 bait vector into yeast

(C) Coimmunoprecipitation analysis. Leaf protein extracts were prepared from transgenic *WRKY33-TAP* plants 24 h after infiltration with agrobacteria harboring the *SIB1-4xmyc* (SIB1-myc; lanes 1 and 4), *SIB1/VQmut-4xmyc* (VQmut-myc; lane 2), or *SIB1/NLSmut-4xmyc* (NLSmut-myc; lane 3) construct. The protein complexes were eluted after TAP purification and analyzed by immunoblotting using anti-myc tag antibody. Protein input for WRKY33-TAP and myc-tag SIB1 proteins in the immunoprecipitated complexes is also shown. As a control, coimmunoprecipitation was also performed with untransformed plants after infiltration with agrobacteria harboring *SIB1-4xmyc* (SIB1-myc; lane 5).

cells. Expression of the bait (WRKY33) and prey (SIB1) proteins in yeast cells was confirmed by immunoblotting with anti-myc and anti-FLAG tag antibodies, respectively (see Supplemental Figure 2A online). Expression of the *LacZ* reporter gene was then assessed by assaying of β-galactosidase activity in the protein extracts of transformed yeast cells. These experiments indicated little or no expression of the reporter gene in yeast cells harboring both the mutant SIB1$^{V62A/Q63A}$ prey and WRKY33 bait vectors (Figure 3A). We also infiltrated the transgenic *WRKY33-TAP* plants with agrobacterial cells containing the mutant SIB1$^{V62A/Q63A}$ tag construct (*SIB1/VQmut-4xmyc*). The protein complexes purified from transgenic *WRKY33-TAP* plants infiltrated with the *SIB1/VQmut-4xmyc*–containing agrobacteria generated no cross-reactivity to the anti-myc tag antisera (Figure 2C). These results provide strong evidence that the VQ motif in SIB1 is required for interaction with WRKY33. However, the V62A/Q63A substitutions did not alter the subcellular localization of SIB1 (see Supplemental Figure 1B online).

Failure of MPK4 to Interact with SIB1 or SIB2 in Yeast

MPK4 interacts with and phosphorylates MKS1, which, in turn, interacts with WRKY33 (Andreasson et al., 2005). It was recently reported that MPK4 forms a complex with WRKY33, probably through MKS1, in uninduced cells and releases the transcription factor to activate such defense genes as *PAD3* upon infection of pathogens or treatment with an elicitor (Andreasson et al., 2005). Since WRKY33 also interacts with SIB1 and SIB2, we analyzed the possible interaction of the two SIB proteins with MPK4. Full-length *MPK4* was fused with the BD-myc domain in the modified bait vector and cotransformed with the SIB prey vectors into yeast cells. Expression of the proteins in yeast was again analyzed by immunoblotting (see Supplemental Figure 2B on line). Expression of the *LacZ* reporter gene was then assessed by assaying of LacZ activity in the protein extracts of transformed yeast cells. These experiments indicated little expression of the reporter gene in yeast cells harboring both the SIB prey and MPK4 bait vectors (Figure 3B). By contrast, when the BD-myc-MPK4 bait construct was cotransformed with the AD-FLAG-MKS1 prey construct into yeast cells, expression of the *LacZ* reporter gene was activated (Figure 3B).

Recognition of the C-Terminal WRKY Domain of WRKY33 by SIB1 and SIB2

Next, we set out to map the region of WRKY33 that interacts with SIB1. We generated WRKY33 deletion constructs and fused them with Gal4 BD-myc in the bait vector (Figure 4). These bait constructs were then cotransformed with the SIB1 prey vector into yeast. The expression of both the bait and prey proteins and of the LacZ reporter gene were assessed (Figure 4; see Supplemental Figure 2C online). As described earlier, the truncated WRKY33 protein used in yeast two-hybrid screens was the C-terminal two-thirds of WRKY33 (W33Δ1; amino acids 181 to 519) (Figure 4A). Within the truncated protein are two WRKY domains, with the first between amino acid residues 189 and 239 and the second between residues 367 and 417 (the Trp residue of the conserved WRKYGQK sequence is designed as the starting residue and the second His residue of the C2H2 zinc finger as the last residue of a WRKY domain). As shown in Figure 4A, deletion of the C-terminal 97 residues (W33Δ2; amino acids 181 to 422) had little effect on the ability of WRKY33 to interact with SIB1. This result indicated that the BD of WRKY33 is located in the middle of the protein, in the region spanning the two WRKY domains. Additional mapping showed that the N-terminal WRKY domain and most of the region between the two WRKY domains of WRKY33 were not required for interaction with SIB1 (Figure 4A). On the other hand, the region between amino acid residues 331 and 422 (W33Δ7) was active in interaction with SIB1 (Figure 4A). This region contains the second (C-terminal) WRKY domain plus 36 N-terminal and four C-terminal residues (W33Δ7). These results pointed to a critical role of the C-terminal WRKY domain of WRKY33 in the interaction with the VQ motif–containing protein.

To determine whether the whole C-terminal WRKY domain is required for interaction, we generated additional truncated WRKY33 constructs. First, we deleted the C-terminal seven residues of W33Δ7, which include the two conserved His residues in the zinc-finger motif, and found the resulting protein (W33Δ8; amino acids 331 to 415) to be incapable of interacting with SIB1 (Figure 4B). Second, we deleted the N-terminal 20 residues of W33Δ7 and found that the resulting protein (W33Δ9; amino acids 351 to 422) failed to interact with SIB1 (Figure 4B). Interestingly, W33Δ10 (amino acids 351 to 519), which differs from W33Δ9 by an additional 97 residues at the C terminus, interacted with SIB1, based on the substantial activity of the LacZ reporter (Figure 4B). Third, to determine whether the interaction is really dependent on the WRKY domain or is conditioned by a critical size of the WRKY domain, we generated another WRKY33 construct (W33Δ11), which is identical to W33Δ7 in size (amino acid 331 to amino acid 422) but has the two conserved His residues in the zinc-finger motif mutated to Ala residues (Figure 4B). However, unlike W33Δ7, W33Δ11 failed to interact with SIB1 (Figure 4B). We also tested these same truncated WRKY33 proteins for interactions with SIB2 and MKS1, with similar results (Figure 4). Thus, the interaction of WRKY33 with SIB1, SIB2, and MKS1 requires not only the entire second (C-terminal) WRKY domain but also a substantial number of amino acid residues flanking the zinc-finger motif.

Failure of SIB1 and SIB2 to Interact with Group II or III WRKY Proteins

Based on the number and structures of the conserved WRKY zinc-finger motifs, WRKY proteins can be classified into three groups (Rushton et al., 2010). WRKY33 and closely related WRKY25 belong to the first group, with two Cys2His2 zinc-finger motifs. Several other characterized *Arabidopsis* WRKY proteins, including WRKY18, are members of the second group, containing one Cys2His2 zinc-finger motif, while others, such as WRKY70, are members of the third group, with one Cys2HisCys zinc-finger motif (Dong et al., 2003). To determine the specificity of SIB1 interaction with WRKY proteins, we tested WRKY25, WRKY18, and WRKY70. For WRKY25, a group I WRKY protein, we first generated a truncated protein comprising the C-terminal WRKY domain plus 30 and 20 amino acid residues at the N- and C-terminal sides of the zinc-finger motif, respectively. Likewise,

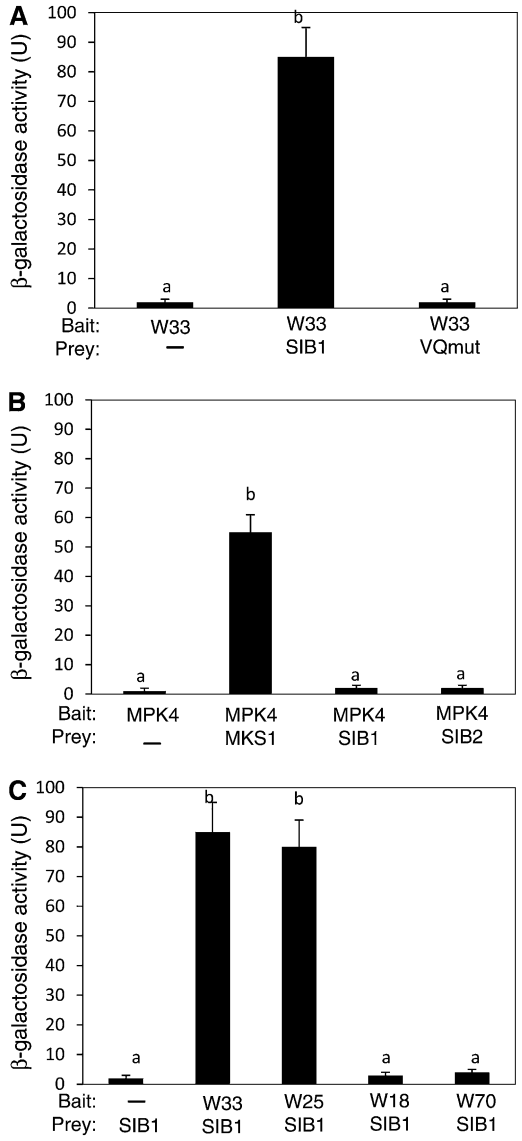

Figure 3. Specificity of Protein–Protein Interactions in Yeast Cells.

(A) The importance of the VQ motif of SIB1 for interaction with WRKY33. The myc-tagged Gal4 DNA BD–WRKY33 (W33) fusion bait vector was cotransformed with FLAG-tagged activation domain–SIB1 (SIB1) or -SIB1$^{V62A/Q63A}$ (VQmut) fusion prey vector into yeast cells and assayed for *LacZ* reporter gene expression. The empty pAD prey vector (–) was used as negative control.

(B) MPK4 interaction with MKS1 but not with SIB1 or SIB2. The myc-tagged Gal4 DNA BD–MPK4 (MPK4) fusion bait vector was cotransformed with FLAG-tagged activation domain-MKS1 (MKS1), -SIB1 (SIB1), or -SIB2 (SIB2) fusion prey vector into yeast cells and assayed for *LacZ* reporter gene expression. The empty pAD prey vector (–) was used as negative control.

(C) SIB1 interaction with WRKY33 and WRKY25 but not with WRKY18 or WRKY70. The Gal4 DNA BD–WRKY33 (W33), -WRKY25 (W25), -WRKY18 (W18), or -WRKY70 (W70) fusion bait vector was cotransformed with AD-SIB1 (SIB1) fusion prey vector into yeast cells and assayed for *LacZ* reporter gene expression. The empty pBD prey vector (–) was used as negative control.

truncated *WRKY18* or *WRKY70* were also generated, fused with the BD-myc domain of Gal4 in the bait vector and cotransformed with the SIB1 prey vector into yeast cells. The expressed proteins were detected by immunoblotting (see Supplemental Figure 2D online). Direct assay of LacZ activity indicated that SIB1 interacted with the C-terminal WRKY domain of the group I WRKY25 protein but not with that of the group II WRKY18 or group III WRKY70 protein (Figure 3C).

Stimulation of DNA Binding Activity of WRKY33 by SIB1 and SIB2

In WRKY proteins, such as WRKY33, that contain two WRKY domains, the C-terminal domain is primarily responsible for DNA binding (Ishiguro and Nakamura, 1994; de Pater et al., 1996). It is therefore possible that binding of SIBs and MKS1 to the C-terminal WRKY domain of WRKY33 affects its DNA binding activity. To test this possibility, we expressed the genes encoding SIBs and MKS1 in *Escherichia coli*, purified the recombinant proteins, and tested their effects on WRKY33 binding to a DNA probe containing two TTGACC W boxes (Pchn0; Figure 5A) using the electrophoretic mobility shift assay (EMSA). In the absence of WRKY33, these VQ motif–containing proteins did not bind to the DNA probe (Figure 5B). As previously reported (Zheng et al., 2006), WRKY33 recognized the DNA probe based on the formation of specific protein-DNA complexes with reduced migration in EMSA (Figure 5B). When the W-box sequences in the oligo probes were mutated from TTGACC to TTGAAC (mPchn0; Figure 5A), the binding complexes were not detected (Figure 5B). These results suggest that recombinant WRKY33 protein specifically binds to the W-box sequences in the synthesized probe. When SIB1, SIB2, and MKS1 were added to the DNA probe and WRKY33 mixture, we observed formation of supershifted protein-DNA complexes in EMSA (Figure 5B). Furthermore, the intensities of the protein-DNA bands were substantially enhanced when SIB1, MKS1, and SIB2 were included in the binding mixture (Figure 5B). By contrast, inclusion of BSA or the SIB1$^{V234A/Q235A}$ mutant protein (VQmut) did not cause supershifting or enhance intensity of the protein-DNA complexes (Figure 5B). Thus, the three VQ motif–containing proteins recognized the DNA binding WRKY domain and stimulated the DNA binding activity of WRKY33.

To determine whether SIB1 was present in the supershifted WRKY33/DNA complexes, we generated SIB1-myc recombinant proteins and found that the tagged protein was as effective as SIB1 in stimulating the DNA binding activity of WRKY33 (see Supplemental Figure 3 online). Furthermore, when the anti-myc antibody was included in the binding mixture, we observed

Expression of the bait and prey proteins in yeast cells was analyzed by immunoblotting using anti-myc or anti-FLAG tag antibody (see Supplemental Figures 2A, 2B, and 2D online). Means and standard errors for LacZ β-galactosidase activity were calculated from five separate colonies per construct used in the assays that used ONPG as substrate. According to Duncan's multiple range test (P = 0.05), means of the units (U) of β-galactosidase activity do not differ significantly if they are indicated with the same letter.

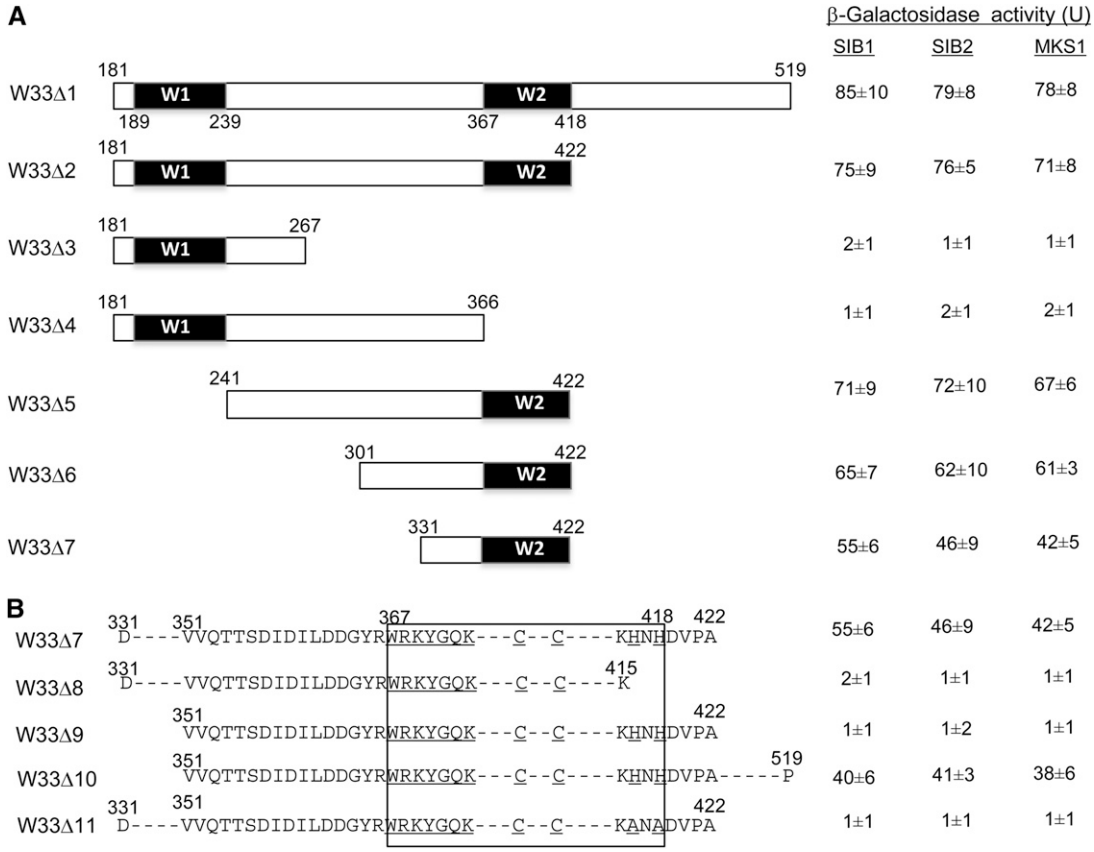

Figure 4. Mapping of the Interaction Domain of WRKY33 with SIB1, SIB2, and MKS1.

WRKY33 deletion constructs for various subregions **(A)** or the C-terminal WRKY domain **(B)** of WRKY33 were inserted into the pBD-myc-Gal4 fusion vector and cotransformed into yeast cells with pAD-FLAG-SIB1. The numbers of the amino acid residues in these truncated WRKY33 proteins are indicated. Yeast transformants were analyzed for *LacZ* reporter gene expression through assays of β-galactosidase activity using ONPG as a substrate. Five separate colonies per construct were used for assays of LacZ β-galactosidase activity. Expression of bait and prey proteins in yeast cells was analyzed by immunoblotting using anti-myc or anti-FLAG tag antibody (see Supplemental Figure 2C online).

further shifting of the WRKY33/DNA bands in EMSA (see Supplemental Figure 3 online). This result strongly suggested that SIB1 was present in the supershifted WRKY33/DNA complexes.

SIB1 Does Not Significantly Affect the Transcription-Activating Activity of WRKY33

As a transcription factor, WRKY33 likely has a transcription-activating or -repressing activity, in addition to the sequence-specific DNA binding activity. Through binding to its C-terminal WRKY domain, SIB proteins may not only affect the DNA binding activity but also modulate the transcription-regulating activity of WRKY33 through a variety of means. To test this possibility, we first determined the transcription-regulating activity of WRKY33 using a stable transgenic reporter/effector system previously used for the analysis of several other *Arabidopsis* WRKY proteins (Kim et al., 2006, 2008; Xing et al., 2008). In this system, a β-glucuronidase (*GUS*) reporter gene is driven by a synthetic promoter consisting of the −100 *CaMV 35S* promoter and eight copies of the *LexA* operator sequence (Figure 6A). Under control of the minimal *CaMV 35S* promoter, the *GUS* reporter gene is constitutively expressed at low levels, thereby making it suitable for assays of transcription activation or repression by determining an increase or decrease in GUS activities following coexpression of an effector protein.

To generate the WRKY33 effector, we fused its coding region with the DNA binding domain (DBD) of LexA (Figure 5A). The WRKY33-DBD fusion was placed behind the dexamethasone (DEX)-inducible *Gal4* promoter in *pTA7002* (Aoyama and Chua, 1997) and transformed into plants already containing the *GUS* reporter gene. As controls, unfused WRKY33 and LexA DBD under the control of the same inducible promoter (Figure 6A) were also transformed into the transgenic *GUS* reporter plants as controls. To determine how an expressed effector affects the GUS reporter gene, we determined the change of GUS activity in the transgenic plants as a result of induction of the effector gene expression following spraying with 20 μM DEX. In transgenic plants containing the unfused *WRKY33* or *LexA DBD* effector gene, their induction after DEX spraying did not change the GUS activities (Figure 6B). In transgenic plants containing the LexA

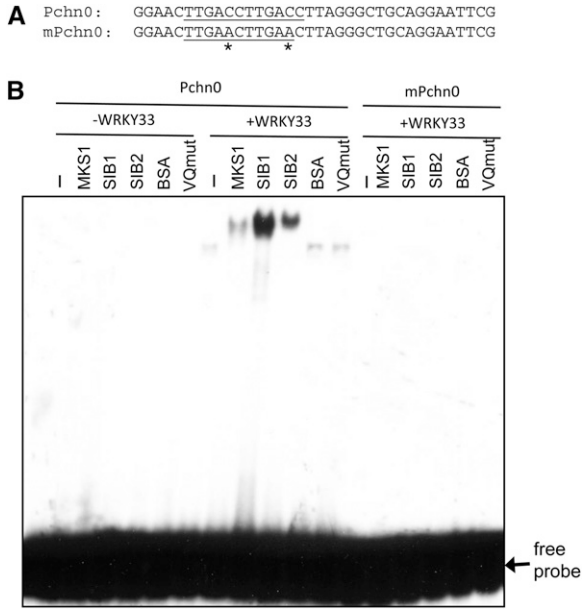

Figure 5. SIB1 Stimulates the DNA Binding Activity of WRKY33.

(A) Oligonucleotides used in the EMSA. The Pchn0 probe contains two direct W-box repeats, while in the mPchn0 probe, the TTGACC sequences are mutated to TTGAAC. The wild-type and mutated W-box sequences are underlined.

(B) EMSA of the effects of interacting proteins on binding of WRKY33 to the W-box (TTGACT) sequences. Recombinant WRKY33, SIB1, SIB2, MKS1, and SIB1$^{V62A/Q63A}$ (VQmut) were purified from *E. coli* cells and used for DNA binding assays with Pchn0 and mPchn0 as probes. The binding reactions (20 μL) contained 2 ng labeled oligo DNA, 5 μg polydeoxyinosinic-deoxycytidylic acid, and 0.5 μg recombinant protein. BSA was included as negative control. The binding assays were repeated twice with independently prepared recombinant proteins with similar results.

DBD-WRKY33 effector, its induction after DEX treatment resulted in an ~2.6-fold increase in GUS activity (Figure 6B). Thus, WRKY33 acts as a transcriptional activator in plant cells.

To determine the effect of SIB1 on the transcription-activating activity of WRKY33, we transformed the transgenic *WRKY33* effector/*GUS* reporter plants with a *SIB1* overexpression construct under control of the *CaMV 35S* promoter. Transgenic plants harboring the *SIB1* overexpression construct were identified by their resistance to the Basta herbicide, and *SIB1*-overexpressing lines were identified by RNA gel blotting analysis (see Supplemental Figure 4 online). As described earlier, in the transgenic lines not overexpressing *SIB1*, induced expression of the fused LexA-WRKY33 effector resulted in about a 2.6-fold induction in GUS activity (Figure 6B). In the transgenic *SIB1*-overexpressing lines, we observed a 2.45-fold induction of GUS after DEX treatment (Figure 6B). Thus, SIB1 overexpression did not significantly affect the transcription-activating activity of WRKY33.

Induction of *SIB1* and *SIB2* by *B. cinerea*

SIB1 and *SIB2* are both upregulated by light (Morikawa et al., 2002). To analyze their role in plant defense against necrotrophic pathogens, we first examined their expression in response to *B. cinerea*. Transcripts of the two genes were detected in plants before infection (Figure 7). After being sprayed with a buffer or *B. cinerea* spores, plants were covered with a plastic dome to maintain high humidity, and this treatment reduced the expression of *SIB1* and *SIB2* (Figure 7), likely due to reduced light. In buffer-sprayed plants, *SIB1* and *SIB2* transcript levels remained relatively low throughout the 3-d period (Figure 6). In *B. cinerea*–infected plants, the transcript levels of *SIB1* and *SIB2* were markedly enhanced, similar to those of *WRKY33* (Figure 7). *SIB1* is also induced by SA and the bacterial pathogen *P. syringae* (Narusaka et al., 2008; Xie et al., 2010). Pathogen-induced

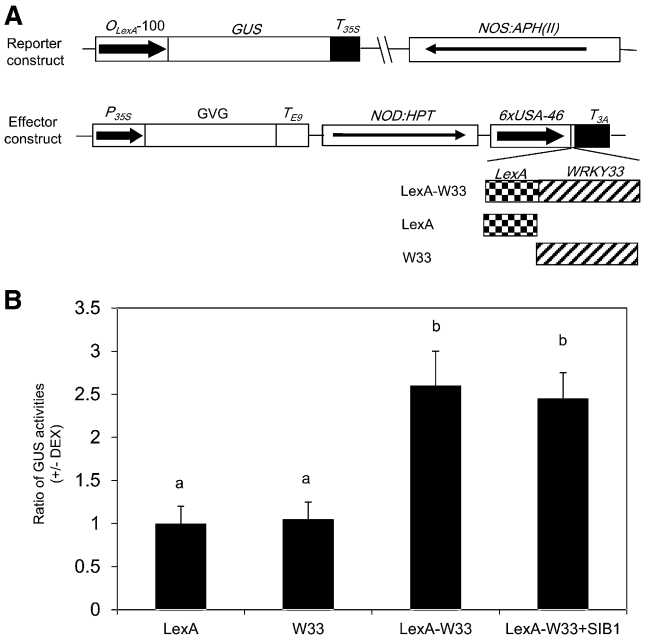

Figure 6. Effect of SIB1 on Transcription-Activating Activity of WRKY33.

(A) Constructs of reporter and effector genes. The *GUS* reporter gene is driven by a synthetic promoter consisting of the −100 minimal *CaMV 35S* promoter and eight copies of the *LexA* operator sequence (O_{LexA}-*100*). The effector genes were cloned into pTA7002 behind the steroid-inducible promoter. The three effector genes encode LexADBA-WRKY33 fusion protein (LexA-W33), LexA DBD (LexA), and WRKY33 (W33), respectively. The thick and thin arrows indicate the directions of promoters and selection markers in the constructs, respectively.

(B) The effect of overexpressed SIB1 on the transcriptional activation activity of WRKY33. A *SIB1*-overexpressing line was crossed to three independent lines harboring both the *GUS* reporter and the LexA-W33 effector. A transgenic line containing an empty vector was also crossed to the same *GUS* LexA-W33 effector double transformant and used as the control. The ratios of GUS activities were calculated from the GUS activities determined in the leaves harvested 18 h after DEX treatment (+) over those determined prior to DEX treatment (−). The means and standard errors were calculated from three lines (10 plants per line) for each effector. Expression of *LexA*, *LexA-WRKY33*, and *SIB1* in the transgenic lines was confirmed by RNA gel blotting (see Supplemental Figure 4 online). According to Duncan's multiple range test (P = 0.05), means of the ratios of GUS activities do not differ significantly if they are indicated with the same letter.

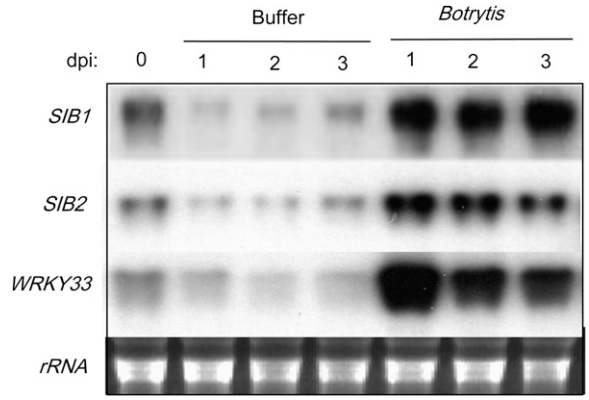

Figure 7. Expression of *SIB1*, *SIB2*, and *WRKY33* in Response to *B. cinerea*.

Plants were inoculated with *B. cinerea* as described in Methods. The inoculated leaves were collected at the indicated days after inoculation (dpi) for RNA isolation. RNA gel blot analysis was performed with ^{32}P-labeled *SIB1*, *SIB2*, and *WRKY33*. Ethidium bromide staining of rRNA is shown for the assessment of equal loading. The experiments were repeated three times with similar results. WT, wild type.

expression of *SIB1* and *SIB2* supports their involvement in plant defense.

Compromised Resistance of *sib* Mutants to *B. cinerea*

Given the observed interaction with WRKY33 and induced expression by *B. cinerea*, we further investigated the role of both SIB1 and SIB2 in plant disease resistance using knockout or RNA interference (RNAi) mutants. We identified two transposon-tagged lines (*sib1-3*, SM_3.30601; *sib1-4*, SM_3.30596) for *SIB1* and a transposon-tagged line for *SIB2* (*sib2-1*, SM_3_16236). These *sib1* and *sib2* mutants contain the transposon insertion in the middle of their respective genes (see Supplemental Figure 5A online). RT-PCR failed to detect accumulation of transcripts for the respective genes in the mutants using primers flanking the insertion sites (see Supplemental Figure 5B online), indicating that transposon insertions disrupt the open reading frame. As there is only a single *sib2* knockout mutant, we generated transgenic *sib2* RNAi knockdown lines with reduced *SIB2* expression. To determine possible functional redundancy, we also generated two double mutants (*sib1-3 sib2-1* and *sib1-4 sib2-1*) through genetic crossing. These knockout or knockdown single and double mutants grew and developed normally and exhibited no significant morphological phenotypes when compared with wild-type plants.

These mutants were first spray inoculated with *B. cinerea* and compared for disease symptoms and pathogen growth with wild-type and *wrky33* mutant plants. In spray-inoculated wild-type plants, *B. cinerea* infection caused small necrotic spots and minor chlorosis that did not spread significantly to cause extensive tissue damage (Figure 8A). As a result, the majority of leaves from the wild-type plants remained green at 4 d after inoculation (DAI). In the *wrky33* mutant, the necrotic spots and chlorosis spread rapidly, and a majority of leaves were macerated at 4 DAI (Figure 8A). In spray-inoculated *sib1* and *sib2* single mutants, the necrotrophic spots spread substantially and by 4 DAI, a substantial portion of old leaves exhibited chlorosis or maceration (Figure 8A). The spread of necrosis and leaf maceration were significantly greater in the *sib1 sib2* double mutant plants after *B. cinerea* infection than those in the single mutants (Figure 8A). However, the extent of leaf maceration in the *sib* single and double mutants, while more severe than that of the wild type, was substantially less than that of the *wrky33* mutant (Figure 8A).

To determine whether disease symptoms were correlated with pathogen growth, we analyzed the accumulation of the *B. cinerea ActinA* (*BcActA*) transcript as a measure of fungal growth in inoculated plants. The transcript levels of the constitutively expressed fungal gene correlated with fungal biomass (Benito et al., 1998). Total RNA was isolated from infected plants at 4 DAI and blotted and probed with a *BcActA* gene fragment (Benito

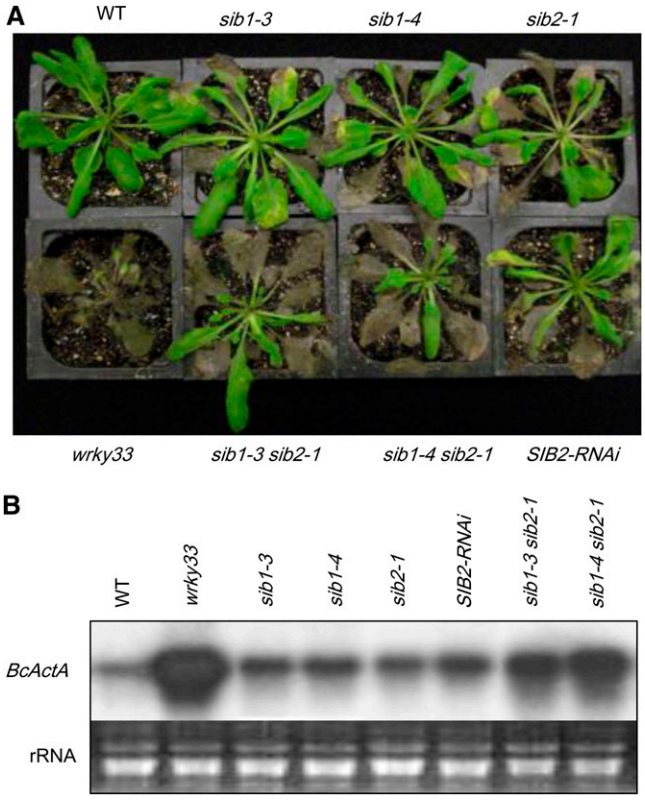

Figure 8. Responses of Loss-of-Function Mutants to *B. cinerea*.

(A) Responses to *B. cinerea* using whole-plant inoculation. Col-0 wild-type, *wrky33*, *sib1*, *sib2*, and *sib1 sib2* mutants, and *SIB2-RNAi* plants were inoculated by spraying spore suspension at a density of 2.5×10^5 spores/mL and kept at high humidity. Photographs of representative plants were taken 4 d after inoculation

(B) Estimation of the biomass of the fungal pathogen on infected plants. Total RNA was isolated from the plants 4 d after inoculation and probed with a *B. cinerea Actin* gene probe to determine the biomass of the fungal pathogen on infected plants. The experiments were repeated at least three times with similar results.

et al., 1998). As previously reported (Zheng et al., 2006), substantially higher levels of the fungal *ActA* gene transcript were detected in the *wrky33* mutant plants than in the wild type after *B. cinerea* infection (Figure 8B). *B. cinerea ActA* gene transcript levels were also significantly increased in the *sib1* and *sib2* single mutants and, to a greater extent, in the *sib1 sib2* double mutants (Figure 8B). Quantitative real-time PCR (qRT-PCR) confirmed the increased accumulation of the fungal gene transcripts in the mutant plants (see Supplemental Figure 6A online). Thus, both symptom development and fungal growth indicated that the *sib* mutant plants were compromised in resistance to *B. cinerea*.

Enhancement of Resistance to *B. cinerea* by Constitutive Overexpression of *SIB1*

To complement the loss-of-function approach for functional analysis of the *SIB* genes, we examined the effect of *SIB1* overexpression on resistance to *B. cinerea*. We generated plants containing a full-length *SIB1* cDNA driven by the *CaMV 35S* promoter (*35S*:*SIB1*) (Figure 9A). RNA gel blotting identified transgenic plants that contained constitutively elevated levels of *SIB1* transcript. For further study, we chose two transgenic lines (L2 and L5) that constitutively expressed *SIB1* at elevated levels (see Supplemental Figure 7 online) and contain a single T-DNA locus in their genomes, based on the ratio of antibiotic resistance phenotypes. Analysis of F3 homozygous plants from both lines revealed no major difference in growth or development from that of wild-type plants, although they appeared to be slightly but significantly smaller. Following inoculation with *B. cinerea*, the transgenic *35S*:*SIB1* overexpression lines showed significantly reduced disease symptoms with highly restricted disease lesions and contained reduced biomass of *B. cinerea* when compared with wild-type plants (Figure 9B). Thus, overexpression of *SIB1* increased resistance to *B. cinerea.* This result supports the notion that the WRKY33-interacting partner plays an important role in plant defense against the necrotrophic pathogen.

Chloroplast Targeting Signal Peptide of SIB1 Is Dispensable for Enhancing Resistance to *B. cinerea*

SIB1 is dual targeted to both chloroplasts and the nucleus; therefore, the enhanced resistance to *B. cinerea* in the *SIB1* overexpression lines could be attributed to its action in chloroplasts, the nucleus, or both. To distinguish among these possibilities, we deleted the DNA sequence corresponding to the N-terminal chloroplast-targeting signal peptide of SIB1 and overexpressed the truncated gene (*SIB1ΔSP*) under control of the *CaMV 35S* promoter in *Arabidopsis* plants (Figure 9A). Transgenic plants constitutively overexpressing *SIB1ΔSP* were identified through RNA gel blotting (see Supplemental Figure 7 online) and tested for response to *B. cinerea*. As shown in Figure 9B, the transgenic *SIB1ΔSP*-overexpressing plants were as resistant as the *SIB1*-overexpressing plants to the necrotrophic pathogen. This result strongly suggests that the chloroplast targeting signal peptide of SIB1 is not important for its role in plant resistance to necrotrophic pathogens. BiFC analysis indicated that SIB1ΔSP interacts with WRKY33 normally in plant cells (see Supplemental Figure 1A online).

The VQ Motif and NLS of SIB1 Are Important for Enhancing Resistance to *B. cinerea*

The VQ motif and the putative NLS of SIB1 are both important for the interaction with WRKY33 in plant cells (Figure 2C). To determine the role of the motifs in the ability of SIB1 to enhance disease resistance, we overexpressed the *SIB1/VQmut* and *SIB1/NLSmut* genes under the *CaMV 35S* promoter in *Arabidopsis* plants. Transgenic lines overexpressing the mutant *SIB1* genes were identified using RNA gel blotting (see Supplemental Figure 7 online) and tested for response to *B. cinerea*. Unlike the highly resistant transgenic *SIB1*- or *SIB1ΔSP*-overexpressing plants, transgenic plants overexpressing *SIB1/VQmut* or *SIB1/NLSmut* were as susceptible as wild-type plants to the fungal pathogen (Figure 9B). Thus, the VQ motif and the putative NLS are both critical for SIB1's activity in enhancing resistance to the necrotrophic pathogen.

SIB1-Enhanced Resistance to *B. cinerea* Is WRKY33 Dependent

SIB1 interacts with WRKY33 in the nucleus (Figure 2) but is also targeted to the chloroplast and interacts with SIG1, according to both yeast two-hybrid and in vitro pull-down assays (Morikawa et al., 2002). Overexpression of not only the full-length SIB1 but also truncated SIB1ΔSP led to enhanced resistance to *B. cinerea* (Figure 9B), suggesting that the role of SIB1 in plant resistance to *B. cinerea* is mediated by its interaction with WRKY33 in the nucleus. To further test this, we examined whether enhanced *B. cinerea* resistance of *SIB1*-overexpressing plants is WRKY33 dependent. We introduced the *SIB1*-overexpressing construct into the *wrky33* mutant plants. Transformant lines overexpressing *SIB1* at high levels in the *wrky33* mutant background were identified by RNA gel blotting (see Supplemental Figure 7 online) and analyzed for their response to *B. cinerea*. As shown in Figure 9C, unlike the transgenic *SIB1*-overexpressing lines in the wild-type background, which were highly resistant to *B. cinerea*, the two *SIB1*-overexpressing lines in the *wrky33* mutant background were highly susceptible to the necrotrophic pathogen. Thus, WRKY33 is important for SIB1-conferred resistance to *B. cinerea*.

Regulation of *PDF1.2* by SIB Proteins

JA-mediated defense plays an important role in regulating the expression of plant defense genes and resistance to necrotrophic pathogens. We have previously shown that enhanced susceptibility of *wrky33* mutants to *B. cinerea* is associated with reduced expression of JA-regulated *PDF1.2* expression in *B. cinerea*–infected plants (Zheng et al., 2006). To determine whether the effects of the mutations or overexpression of *SIB1* genes on plant resistance to *B. cinerea* is also associated with altered JA-mediated defense, we examined the expression of the JA-regulated *PDF1.2* defensin gene after *B. cinerea* infection. *PDF1.2* expression was induced in wild-type plants in response

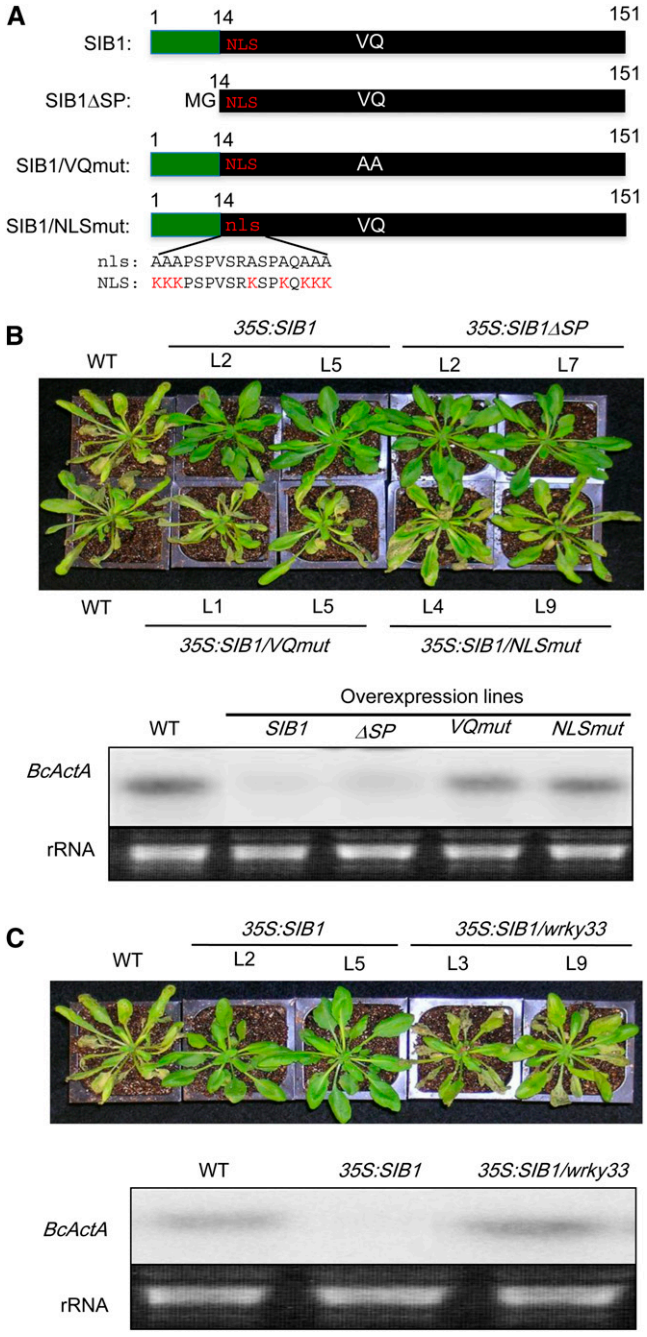

Figure 9. Responses of *SIB1*-Overexpressing Lines to *B. cinerea*.

(A) Diagrams of the full-length SIB1, truncated SIB1 lacking the N-terminal chloroplast targeting signal peptide (SIB1ΔSP), SIB1$^{V62A/Q63A}$ (SIB1/VQmut), and SIB1 with all the Lys (K) residues in the putative NLS changed to Ala (A) residues (SIB1/NLSmut). The numbers of the amino acid residues and the two amino acid residues (MG) added to the N terminus of SIB1ΔSP are indicated. The DNA fragments corresponding to the proteins were inserted behind the *CaMV 35S* promoter in a plant transformation vector.

(B) Responses of *SIB1*, *SIB1ΔSP*, *SIB1/VQmut*, or *SIB1/NLSmut*-overexpressing lines to *B. cinerea*. Two transgenic lines for each transgene that expressed similar levels of *SIB1* were identified by RNA gel blot analysis (see Supplemental Figure 7 online). Col-0 wild-type (WT) and the transgenic overexpression lines were inoculated by spraying spore suspension at a density of 2.5 × 10^5 spores/mL and kept at high humidity. Photographs of representative plants were taken 5 d after the inoculation **(top)**. The biomass of the fungal pathogen on infected plants was estimated using RNA gel blotting with a *B. cinerea Actin* gene **(bottom)**.

(C) WRKY33 dependency of SIB1-enhanced resistance to *B. cinerea*. The *35:SIB1* construct was transformed into *wrky33* mutant plants, and two transformant lines expressing the *SIB1* transgene at levels similar to those in the two lines in the wild-type background were identified by RNA gel blot analysis (see Supplemental Figure 7 online). Col-0 wild-type and the transgenic overexpression lines were inoculated by spraying spore suspension at a density of 2.5 × 10^5 spores/mL and kept at high humidity. Photographs of representative plants were taken 5 d after the inoculation **(top)**. The biomass of the fungal pathogen on infected plants was estimated using RNA gel blotting with a *B. cinerea Actin* gene **(bottom)**.

to *B. cinerea* infection, but its induction was substantially reduced in the *wrky33* mutant, as previously reported (Figure 10) (Zheng et al., 2006). The induction patterns of *PDF1.2* in the *sib1* and *sib2* mutants were similar to that of wild-type plants. On the other hand, we repeatedly observed reduced *PDF1.2* transcript levels at 1 or 2 DAI in the *sib1 sib2* double mutant plants when compared with those in the wild type (Figure 10). By 3 and 4 DAI, the transcript levels for the defensin gene in the *sib1 sib2* double mutant were similar to those in the wild type (Figure 10). Thus, induction of JA-regulated *PDF.1.2* appeared to be significantly delayed in *B. cinerea*–infected *sib1 sib2* double mutant plants. The delayed induction of *PDF1.2* in *B. cinerea*–infected *sib1 sib2* double mutant plants was confirmed by qRT-PCR (see Supplemental Figure 6B online).

Unlike in the wild type and *wrky33* and *sib* mutants, there were significant basal levels of *PDF1.2* transcripts in uninfected or mock-inoculated *SIB1*-overexpressing plants (Figure 10). In addition, the transcript levels for *PDF1.2* in the *B. cinerea*–infected *SIB1*-overexpressing plants were substantially higher at 1, 2, and 3 DAI than those in *B. cinerea*–infected wild-type plants (Figure 10). These results indicate that like WRKY33, SIB1 has a positive role in the regulation of JA-regulated *PDF1.2* expression.

Functional Analysis of *SIG1* in Plant Defense

To further examine how SIBs regulate plant defense against necrotrophic pathogens, we functionally analyzed SIG1, the chloroplast-interacting partner of SIBs, for possible roles in plant resistance to *B. cinerea*. First, we analyzed the expression of *SIG1* in response to *B. cinerea* infection. As shown in Figure 11A, the transcript levels of *SIG1* were significantly reduced at 1 DAI with either buffer or *B. cinerea*, most likely due to the reduced light intensity caused by the plastic dome that was used to maintain high humidity. The transcript levels of *SIG1* were subsequently recovered to similar levels in both mock- and *B. cinerea*–inoculated plants (Figure 11). Thus, unlike *SIB1* and *SIB2*, *SIG1* was not responsive to *B. cinerea* infection.

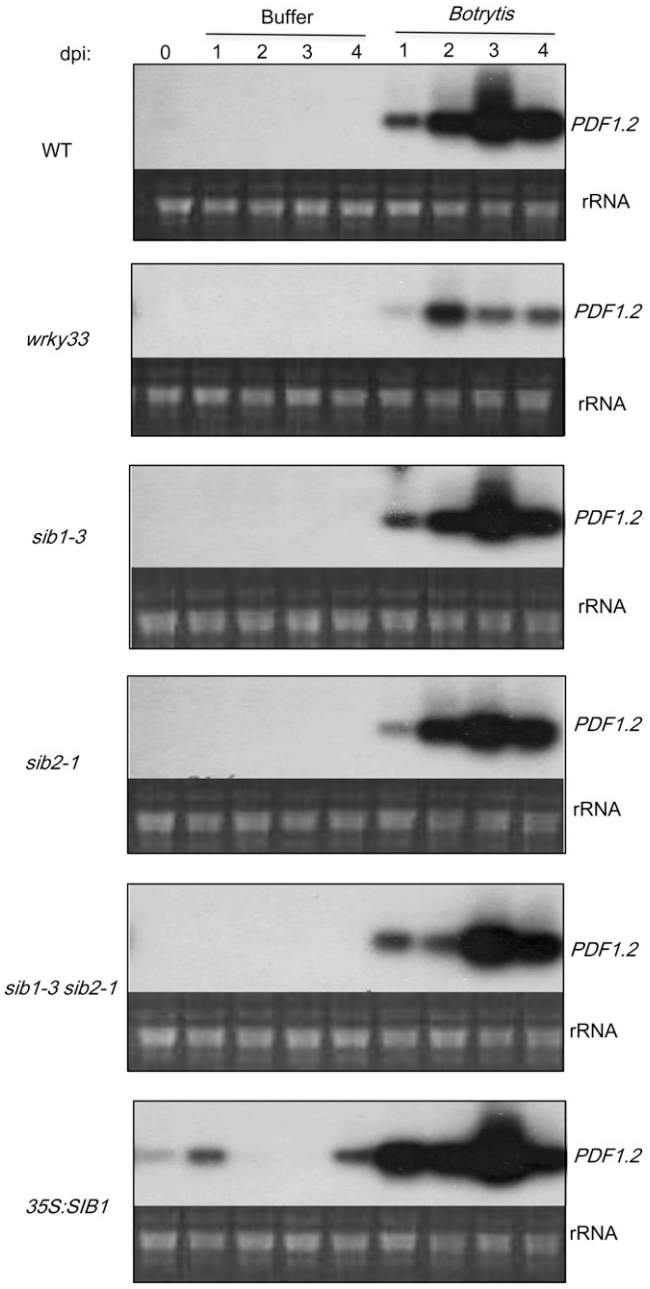

Figure 10. *PDF1.2* Expression after *B. cinerea* Infection.

Col-0 wild-type (WT) or mutant plants were either mock inoculated (Buffer) or inoculated with *B. cinerea*. The inoculated leaves were collected at the indicated days after inoculation (dpi) for RNA isolation. RNA gel blot analysis was performed with a ^{32}P-labeled *PDF1.2* DNA fragment. Ethidium bromide staining of rRNA is shown for the assessment of equal loading. The experiments were repeated twice with similar results.

Second, we identified two independent *sig1* T-DNA insertion mutants. The *sig1-1* (SALK_147985) and *sig1-2* (GABI_758B02) mutants contain a T-DNA insertion in the 9th and 8th exon of *SIG1*, respectively (see Supplemental Figure 5A online). RT-PCR failed to detect transcripts of *SIG1* in the mutant (see Supplemental Figure 5B online). We also generated transgenic *Arabidopsis* plants overexpressing *SIG1* under control of the constitutive *CaMV 35S* promoter (see Supplemental Figure 8 online). As shown in Figure 11B, we observed no significant difference between the wild type and *sig1* mutants in disease symptom development after *B. cinerea* infection. These results suggest that SIG1 does not play a major role in plant resistance to *B. cinerea*.

DISCUSSION

SIB1 and SIB2 as Positive Regulators of WRKY33-Mediated Defense

The *Arabidopsis* WRKY33 transcription factor is important for plant resistance to necrotrophic pathogens (Zheng et al., 2006). In this study, we have shown that WRKY33 interacts with dual-targeted SIB1 and SIB2 (Figures 2B and 2C), in addition to the

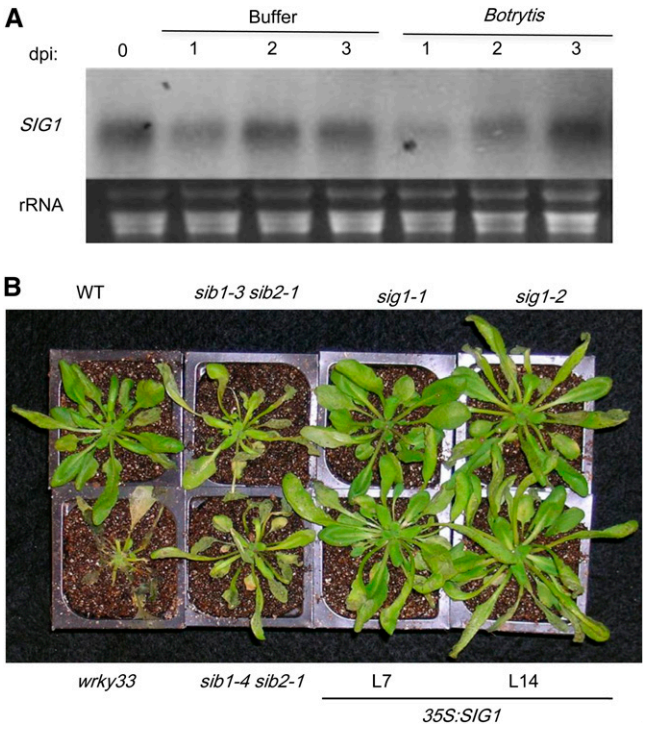

Figure 11. Functional Analysis of SIG1 in Plant Responses to *B. cinerea*.

(A) Expression of *SIG1* in response to *B. cinerea*. Col-0 wild-type plants were either mock inoculated (Buffer) or inoculated with *B. cinerea*. The inoculated leaves were collected at the indicated days after inoculation (dpi) for RNA isolation. RNA gel blot analysis was performed with a ^{32}P-labeled *SIG1* DNA fragment. Ethidium bromide staining of rRNA is shown for the assessment of equal loading.

(B) Responses of *sig1* mutants and *SIG1*-overexpressing plants to *B. cinerea*. Col-0 wild-type (WT), *wrky33*, *sib1 sib2*, and *sig1* mutants and *SIB1*-overexpressing plants were spray inoculated with *B. cinerea* spore suspension at a density of 2.5×10^5 spores/mL and kept at high humidity. Photographs of representative plants were taken 5 d after the inoculation. L, line.

previously identified MKS1 (Andreasson et al., 2005). The three VQ motif–containing proteins recognize the C-terminal WRKY domain and stimulate the DNA binding activity of WRKY33 (Figures 4 and 5). Unlike WRKY33, however, MKS1 appears to affect SA-dependent defense only (Andreasson et al., 2005). Transgenic plants overexpressing *MKS1* accumulated increased levels of SA and SA-regulated *PR1*, *PR2*, and *PR5* transcripts and were hyperresistant to the virulent *Pseudomonas* bacterial pathogen (Andreasson et al., 2005). By contrast, under- or overexpression of *MKS1* had little effect on JA-regulated *PDF1.2* expression (Andreasson et al., 2005), which is often associated with plant defense responses to necrotrophic pathogens. On the other hand, SIB1 and SIB2 play a positive role in plant defense against necrotrophic pathogens. Like *WRKY33*, both *SIB1* and *SIB2* were induced by infection of *B. cinerea*, and the patterns of pathogen-induced expression were similar among the three genes (Figure 7). Thus, WRKY33 and its two DNA binding activators are coordinately regulated during the plant defense response to *B. cinerea*. More importantly, resistance to *B. cinerea* was significantly compromised in the *sib1* and *sib2* mutants (Figure 8) and enhanced in the *SIB1*-overexpressing lines (Figure 9). Mutations and overexpression of *SIB1* and *SIB2* also affected JA-regulated *PDF1.2* expression (Figure 10; see Supplemental Figure 6B online). It should be noted that the phenotypes of even the *sib1 sib2* double knockout mutants in terms of hypersusceptibility to *B. cinerea* and compromised *PDF1.2* expression were not as severe as those of the *wrky33* mutant (Figures 8 and 10). The modest phenotypes of *sib1* and *sib2* mutants indicate that SIB1 and SIB2 play a positively modulating but not essential role in WRKY33-mediated plant defense, consistent with their stimulatory but not essential role for DNA binding of WRKY33 (Figure 5).

Recently, it was reported that two other *sib1* mutants (*sib1-1* and *sib1-2*) responded normally to pathogen infection. However, *sib1-1* (SALK_063337) and *sib1-2* (SALK_127478) mutants contain a T-DNA insertion just upstream of the stop codon and in the upstream promoter region of *SIB1*, respectively. RNA gel blot analysis detected low levels of *SIB1* transcripts in the mutants (Xie et al., 2010), indicating that the mutants are leaky. Interestingly, microarray analysis revealed that even in the *sib1-2* leaky mutant, JA-regulated *PDF1.2* was strongly suppressed at 6 h after *Pseudomonas* infection, while SA-regulated *PR1* and *PR2* transcript levels were not affected (Xie et al., 2010). This observation supports a positive role of SIB1 in JA-mediated defense responses.

Both SIB1 and SIB2 are also targeted to chloroplasts and interact with SIG1, a sigma factor for plastid RNA polymerase. However, transgenic plants overexpressing a truncated SIB1 protein lacking the N-terminal chloroplast targeting signal peptide (SIB1ΔSP) were as resistant to *B. cinerea* as those overexpressing full-length SIB1 (Figure 9B). Thus, deletion of the sequence encoding the SIB1 signal peptide has no effect on the ability of SIB1 to enhance resistance of the plant to *B. cinerea*. We also showed that, unlike *WRKY33*, *SIG1* was unresponsive to *B. cinerea* and its mutations and that overexpression of this gene did not affect plant resistance to *B. cinerea* (Figure 11). Furthermore, *SIB1* overexpression enhanced *B. cinerea* resistance in the wild-type but not in the *wrky33* mutant background (Figure 9C), indicating that the role of SIB1 in plant disease resistance is WRKY33 dependent. These results strongly suggest that the role of SIBs in plant defense is mediated through their interaction with WRKY33 in the nucleus.

While the functional significance of the interactions of SIB1 and SIB2 with chloroplast SIG1 in plant defense was not apparent from our analysis with *B. cinerea*, we are not ruling out their possible roles in plant defense responses under other special conditions. Genetic and molecular analyses have identified genes that encode chloroplast (plastid)-localized proteins involved in the synthesis and signaling of plant defense signal molecules, such as SA and JA. Chloroplasts are also a major source of ROS and redox-active soluble molecules that affect the expression of both chloroplast and nuclear genes associated with defense responses. Interestingly, it has recently been shown that phosphorylation of SIG1 is subject to redox regulation and is important for sustaining balanced expression of components in photosystems I and II through a change in promoter specificity (Shimizu et al., 2010). Interactions with SIB1 and SIB2 might change the specificity of the SIG1 promoter, which could alter the expression of components in photosystems I and II, change the balance of photosynthetic electron transfer, and ultimately affect the production of ROS and redox conditions and plant defense signaling. In addition, it is known that plant resistance to necrotrophic pathogens is strongly influenced by environmental factors such as light (Moor, 1942; Horsfall and Dimond, 1957). During the 1940s, the production of tomato (*Solanum lycopersicum*) seedlings in southern United States for shipment to northern United States developed into a large industry. However, this also introduced the major problem of infection by necrotrophic fungal pathogen *Alternaria solani* because the tomato seedlings were in the dark during shipment (Moor and Thomas, 1943; Rowell, 1953). The induced expression of positive regulators of plant defense, such as SIB1 and SIB2, under light conditions could be an important underlying mechanism for the positive effect of light on plant resistance to necrotrophic pathogens.

Emerging Partnership between Plant WRKY and VQ Motif–Containing Proteins

We have shown that the conserved V and Q residues in the VQ motif of SIB1 are important for its interaction with WRKY33 (Figure 3A). Therefore, the short VQ motif may represent the core of a protein–protein interaction domain. We have also shown that the interaction of WRKY33 with SIB1, SIB2, and MKS1 requires not only the entire C-terminal WRKY domain but also a substantial number of amino acid residues flanking the zinc-finger motif (Figure 4). Zinc fingers are protein structural motifs that coordinate one or more zinc ions to help stabilize their three-dimensional folds as interaction modules usually for binding DNA and proteins. Therefore, the VQ motif–containing proteins may recognize a zinc-bound, folded structure of the C-terminal WRKY domain of WRKY33 to stimulate its DNA binding activity. Although SIB1 overexpression did not significantly affect the transcription-activating activity of WRKY33, it is possible that wild-type levels of SIB1 and related proteins are involved in regulating the transcription-activating activity of WRKY33.

Besides MKS1, SIB1, and SIB2, which interact with WRKY33 and WRKY25, HAIKU1 (IKU1), a VQ motif–containing protein

important for endosperm growth and seed size, has been recently shown to interact with WRKY10 (also known as MINISEED3), a group II WRKY transcription factor that also regulates *Arabidopsis* seed size (Wang et al., 2010). A genomic *IKU1* construct containing mutations in the VQ motif failed to complement the *iku1* mutations, indicating again the important role of the VQ motif for IKU1 (Wang et al., 2010). We recently found that another *Arabidopsis* VQ motif–containing protein (At1G17147) is capable of binding specific WRKY proteins (Z. Lai, unpublished data). In addition, *Arabidopsis* CAMBP25, a VQ motif–containing protein with a negative role in plant osmotic stress responses, is localized in the nucleus (Perruc et al., 2004) and may also function as a regulator of an unknown WRKY protein involved in plant abiotic stress responses. Thus, WRKY and VQ motif–containing proteins can form specific partnership through physical interactions between plant-specific VQ and WRKY motifs.

Plant WRKY proteins are encoded by a large gene superfamily with more than 70 members in *Arabidopsis* (Rushton et al., 2010). Genes encoding WRKY proteins have been identified in low photosynthetic and nonphotosynthetic eukaryotes, but they have greatly proliferated and form large superfamilies only in higher plants (Zhang and Wang, 2005). Likewise, VQ motif–containing proteins are encoded by a large gene family with at least 34 members in *Arabidopsis* (Xie et al., 2010). Genes for VQ domain proteins are found only in the genomes of higher plants and mosses but not in algal genomes (Xie et al., 2010). Thus, the origin of WRKY proteins evolutionarily precedes that of VQ motif–containing proteins. In light of the increasing number of VQ proteins discovered as being WRKY-interacting partners, it is tempting to speculate that proliferation of the VQ gene family might have been, at least in part, evolutionarily driven by the expansion of the WRKY gene family in higher plants.

Genetic and molecular studies over the past decade have revealed that plant WRKY transcription factors regulate diverse biological processes, including plant responses to biotic and abiotic stress, senescence, trichome development, seed development, dormancy, and germination (Rushton et al., 2010). Despite their functional diversity, almost all characterized WRKY proteins recognize the *cis*-acting DNA elements with the minimal consensus TTGACC/T W-box sequence, which is often overrepresented in promoters of many genes associated with plant defense responses (Maleck et al., 2000). Therefore, molecular mechanisms other than DNA binding specificity are important for achieving the functional specificity of WRKY transcription factors. These mechanisms could include differential expression of *WRKY* genes and difference in the transcription-activating or -repressing activity of WRKY proteins. In addition, studies using chromatin immunoprecipitation have shown that the W-box sequences in the promoters of defense genes are constitutively occupied by WRKY proteins even in the absence of pathogen infection or elicitor treatment (Turck et al., 2004). Altered expression of these defense genes upon pathogen infection or elicitor treatment is associated with temporal displacement of WRKY proteins at the promoters by other family members in a stimulus-dependent manner (Turck et al., 2004). Alteration of DNA binding activity of some WRKY proteins upon interactions with VQ motif–containing proteins would facilitate such temporal displacement of WRKY proteins at the promoters of their target genes. Therefore, WRKY-VQ protein partnership may provide an important mechanism for regulating the dynamic functional specificity of WRKY proteins.

VQ domain proteins are in general small (100 to 250) and share diverse amino acid sequences beyond the conserved FXXXVQXXTG motif. In fact, although they all interact with WRKY33, the sequence homology between MKS1 and the two SIB proteins is low. Like MKS1, both SIB1 and SIB2 interact not only with WRKY33 but also with closely related WRKY25 (Andreasson et al., 2005) (Figure 3A). In yeast cells, SIB1 and SIB2 also appear to interact with two other group I WRKY proteins (WRKY3 and WRKY4), albeit at a reduced affinity based on the relatively low levels of *LacZ* reporter gene expression. Thus, SIB1, SIB2, and MKS1 are able to interact with multiple WRKY proteins, and their diverse sequences could affect the dynamic nature of their interactions with different WRKY or other interacting partners, which could explain their distinct biological functions. For example, although MKS1 acts as a WRKY33-interacting partner and stimulates its DNA binding activity, it does not play a significant role in WRKY33-mediated defense against necrotrophic pathogens (Andreasson et al., 2005). Unlike SIB1 and SIB2, MKS1 also interacts with MPK4, which may not release the WRKY33/MKS1 complex in *B. cinerea*–infected plants. In addition, based on its role in SA-dependent defense, MKS1 may interact with other competing WRKY proteins that could reduce or even prevent MKS1 partnership with WRKY33 in *B. cinerea*–infected plants. It should also be noted that, while WRKY33 overexpression has opposite effects to plant resistance to *B. cinerea* and *Pseudomonas* (Zheng et al., 2006), SIB1 overexpression promoted resistance to both pathogens (Xie et al., 2010) (Figure 9). Therefore, there could be additional SIB1-interacting partners that mediate the role of SIB1 in SA-dependent defense. A systematic analysis of plant VQ domain proteins will not only provide important insight into the biological functions of this novel gene family but also generate important information on how plant WRKY proteins regulate the expression of a diverse array of genes and associated biological processes.

METHODS

Plant Growth Conditions

Arabidopsis thaliana plants were grown in growth chambers at 22°C and 120 μE m^{-2} s^{-1} light on a photoperiod of 12 h light and 12 h dark.

Pathogen Inoculation

Growth of *Botrytis cinerea cinerea* strain B05-10 on 2xV8 agar, conidia collection, and spray inoculation using a Preval sprayer were as previously described (Zheng et al., 2006). Inoculated plants were covered with a plastic dome to maintain high humidity, and symptom development was observed 3 to 5 DAI. Biomass of the fungal pathogen was quantified by RNA gel blot analysis of total RNA isolated from inoculated plants for the *B. cinerea Actin* gene transcript levels using a DNA fragment amplified from the *B. cinerea* genome DNA as probe (Mengiste et al., 2003b).

RNA Gel Blot Analysis

Total RNA was isolated from leaves as described (Lagrimini et al., 1987). For RNA gel blot analysis, total RNA (~6 μg) was separated on 1.2%

agarose-formaldehyde gels and blotted to nylon membranes according to standard procedures. Blots were hybridized with [^{32}P]dATP-labeled gene-specific probes. Hybridization was performed in PerfectHyb plus hybridization buffer (Sigma-Aldrich) overnight at 68°C. The membrane was then washed for 15 min twice with 2× SSC (1× SSC is 0.15 M NaCl and 0.015 M sodium citrate) and 1% SDS and for 10 min with 0.1× SSC and 1% SDS at 68°C.

Yeast Two-Hybrid Screening/Assays

WRKY33-interacting proteins were identified using a *Gal4*-based two-hybrid system as described by the manufacturer (Stratagene). Because the full-length WRKY33 protein has transcription-activating activity and activated reporter genes in yeast cells, we used the C-terminal two-thirds of WRKY33 starting from amino acid residue 181 (W33Δ1 in Figure 4A) for yeast two-hybrid screenings. The truncated *WRKY33* gene was PCR amplified and inserted into the *pBD-Gal4* plasmid to generate the bait plasmid. The *Arabidopsis* HybridZAP-2.1 two-hybrid cDNA library was prepared from *Arabidopsis* plants as previously described. The bait plasmid and the cDNA library were used to transform yeast strain YRG-2. Yeast transformants were plated onto selection medium lacking Trp, Leu, and His and confirmed by β-galactosidase activity assays using *o*-nitrophenyl-β-D-galactopyranose (ONPG) as substrate. Plasmid DNA was recovered from positive yeast colonies, transformed into *Escherichia coli* strain DH5α, and isolated for DNA sequencing.

To monitor expressed protein levels in yeast two-hybrid assays, we inserted a *myc* adaptor (5′-AATTGGAACAAAAGCTAATCTCCGAGGAAGACTTGGAATTCGG-3′ and 5′-TCGACCGAATTCCAAGTCTTCCTCGGAGATTAGCTTTTGTTCC-3′) into the *Eco*RI/*Sal*I sites of the pBD-GAL4 bait vector. We also generated a modified pAD-GAL4 prey vector by inserting a FLAG adaptor (5′-AATTGGACTACAAGGACGACGATGACAAGGAATTCCTTC-3′ and 5′-TCGAGAAGGAATTCCTTGTCATCGTCGTCCTTGTAGTCC-3′) into the *Eco*RI/*Xho*I sites. *Arabidopsis* genes or gene fragments tested for protein–protein interaction in yeast cells were PCR amplified and inserted either into the pBD-myc-Gal4 or pAD-FLAG-Gal4 plasmid. The primers used for amplifying these genes or gene fragments include the following: *MKS1* (5′-ATCGAATTCCCAAGTATGGATCCGTCG-3′ and 5′-ATCCTCGAGTCTAATCTTGATCCCAAATATGACT-3′), *MPK4* (5′-ATCGAATTCATGTCGGCGGAGAGTTGTTT-3′ and 5′-ATCGTCGACCACACTGAGTCTTGAGGATTGAA-3′), *WRKY25* (5′-ATCGAATTCGAAGGTGAAGATGAAGGGATGT-3′ and 5′-ATCGTCGACTCACGAGCGACGTAGCGCGGT-3′), *WRKY18* (5′-ATCGAATTCCCTACTGAAACATCGGACAC-3′ and 5′-ATCGTCGACGCTTGTAGCATCCCCTTCAG-3′), and *WRKY70* (5′-ATCGAATTCTCGGAGACGTGTACTATAGAGTCG-3′ and 5′-ATCCTCGAGGGTCACAAGTCTTGCTCTTGG-3′). WRKY33 deletion constructs for mapping of its interaction domain were PCR amplified using the primers listed in Supplemental Table 1 online.

To generate V62A/Q63A substitutions for SIB1, we first amplified a *SIB1* fragment using the following pair of primers: 5′-GTTCAGAGAGCTCGCTGCAGAACTCAC-3′ and 5′-GTAATACGACTCACTATAGGGC-3′. The amplified *SIB1* fragment contains mutations that change the conserved VQ residues into AA residues in the VQ motif. The PCR product was digested with *Sac*I/*Xho*I and fused with the remaining part of *SIB1*. PCR products and cloned products were verified by DNA sequencing. β-Galactosidase activity was assayed according to the manufacturer's manual (Stratagene).

BIFC Assays

DNA sequences of the N-terminal, 173–amino acid, enhanced YFP (N-YFP) and C-terminal, 64–amino acid (C-YFP) fragments were PCR amplified and cloned into pFGC5941 to generate pFGC-N-YFP and pFGC-C-YFP, respectively (Kim et al., 2008). The *WRKY33*, *WRKY18*, and *WRKY48* coding sequences were inserted into pFGC-N-YFP to generate the N-terminal in-frame fusions with N-YFP, whereas *SIB1* and *SIB2* coding sequences were introduced into pFGC-C-YFP to form C-terminal in-frame fusions with C-YFP. The resulting clones were verified through sequencing. The plasmids were introduced into *Agrobacterium tumefaciens* (strain GV3101), and infiltration of *Nicotiana benthamiana* was performed as described previously (Kim et al., 2008). Infected tissues were analyzed at ~24 h after infiltration. Fluorescence and DAPI were visualized using a Zeiss LSM710 confocal microscope, and images were superimposed with Zeiss LSM710 software.

Coimmunoprecipitation

Generation of transgenic plants harboring the *WRKY33-TAP* construct under control of the native WRKY33 promoter has been recently described (Lai et al., 2011). *SIB1/NLSmut* was generated by overlapping PCR using two pairs of primers (5′-TTAGACGCGGCAGCACCATCTCCGGTTTCAAGAGCATCACCAGCGCAAGCGGCGGCGACGACTTCG-3′/5′-TCACATAGAATCGATGCTTCCAAAGT-3′ and 5′-ATGGAGTCATCATCGTCGAC-3′/5′-GGTGCTGCCGCGTCTAAGCTTGTCGTGGTGAGAAAA-3′). Full-length wild-type and mutant *SIB1* genes for the VQ motif (*SIB1/VQmut*) and the putative NLS (*SIB1/NLSmut*) were PCR amplified using primers 5′-AGCCCATGGAGTCATCATCGTCGAC-3′ and 5′-AGCTTAATTAACATAGAATCGATGCTTCCAAAG-3′. The PCR fragments were digested with *Nco*I/*Pac*I and fused with a 4xmyc epitope tag coding sequence at the 3′-end in a modified pFGC5941 binary vector.

For immunoprecipitation experiments, we used *Agrobacterium*-mediated transient expression of *SIB1-4xmyc*, *SIB1/VQmut-4xmyc*, or *SIB1/NLSmut-4xmyc* in the transgenic *WRKY33-TAP Arabidopsis* plants (Lai et al., 2011). The transient expression experiments by agroinfiltration of leaves were performed as previously described (Lee and Yang, 2006). The infiltration induced the *WRKY33-TAP* transgene under the native *WRKY33* promoter, according to the results of both an RNA gel blot and an immunoblot. The infiltrated leaves were collected 24 h later, and protein complexes were purified as we previously described for EDS1-TAP and PAD4-TAP complexes (Xing and Chen, 2006). The protein complexes were eluted and fractionated on a 12.5% SDS-PAGE gel. SIB1-4xmyc, SIB1/VQmut-4xmyc, and SIB1/NLSmut-4xmyc were detected using anti-myc tag antibody (Santa Cruz Biotechnology).

Generation of Transgenic SIB1-GFP Plants

Arabidopsis SIB1 and *SIB1VQmut* full-length cDNAs were PCR amplified and fused to *GFP*. The *SIB1-* and *SIB1VQmut-GFP* fusion genes were subcloned behind the *CaMV 35S* promoter in a binary vector, and *Agrobacterium*-mediated transformation of *Arabidopsis* plants was performed using the floral dip method (Clough and Bent, 1998).

Immunoblot Analysis of Expressed Proteins in Yeast

Total proteins were prepared by boiling yeast cells harboring different constructs at 95°C for 10 min in 50 mM Tris-HCl, pH 8.0,1 mM EDTA, 2% SDS, 12 mM β-mercaptoethanol, and 10 μg/mL PMSF. After the sample was clarified by centrifugation, the proteins were fractionated by SDS-PAGE on a 12.5% polyacrylamide gel, and the separated proteins were electrophoretically transferred to a nitrocellulose filter. Immunoblot analysis was performed using anti-myc or anti-FLAG tag antibody (Santa Cruz Biotechnology) as previously described (Chen et al., 1997).

Recombinant Protein and DNA Binding

The full-length cDNAs of *SIB1*, *SIB2*, *SIB1/VQmut*, *MKS1*, and *WRKY33* were subcloned into the expression vector pET-32a (Novagen) and

transformed into *E. coli* strain BL21 (DE3). To generate SIB1-myc recombinant proteins, we inserted a *myc* adaptor (5′-AATTGGAACAAAAGC-TAATCTCCGAGGAAGACTTGGAATTCGG-3′ and 5′-TCGACCGAATTC-CAAGTCTTCCTCGGAGATTAGCTTTTGTTCC-3′) into the *Eco*RI/*Sal*I sites of pET-32a. Expression of the recombinant proteins was induced by isopropyl β-D-1-thiogalactopyranoside and purified according to the manual provided by Novagen. Purified recombinant proteins were dialyzed overnight against a nuclear extraction buffer (25 mM HEPES/KOH at pH 7.5, 40 mM KCl, 0.1 mM EDTA, 10% glycerol, 1 mM DTT, and 30 mg/L PMSF) at 4°C. Double-stranded synthetic oligonucleotides were labeled to specific activities of ~10^5 cpm/ng using the Klenow fragment of DNA polymerase I. Sequence-specific DNA binding was assayed with EMSA essentially as described previously (Xu et al., 2006).

Assays of Transcriptional Regulatory Activity of WRKY33

Transgenic *Arabidopsis* plants containing a *GUS* reporter gene driven by a synthetic promoter consisting of the −100 minimal *CaMV 35S* promoter and eight copies of the *LexA* operator sequence were previously described (Kim et al., 2006). To generate effector genes, the DNA fragment for the LexA DBD was digested from the plasmid pEG202 (Clontech) using *Hin*dIII and *Eco*RI and cloned into the same sites in pBluescript II KS+. The full-length *WRKY33* cDNA fragment was subsequently subcloned behind the *LexA DBD* to generate a translational fusion. The *LexA DBD-WRKY33* fusion gene was cloned into the *Xho*I and *Spe*I sites of pTA2002 behind the steroid-inducible promoter (Aoyama and Chua, 1997). As controls, unfused *LexA DBD* and *WRKY33* were also cloned into the same sites of pTA7002. These effector constructs were directly transformed into the transgenic *GUS* reporter plants, and double transformants were identified through screening for antibiotic (hygromycin) resistance. Three independent plants (lines) expressing representative levels of the effector gene were identified. The three transgenic lines harboring the *LexW33-WRKY* effector construct were also crossed with a *SIB1*-overexpressing line. The progeny of these transgenic plants were screened for the *GUS* reporter gene using PCR and for effector gene expression using RNA gel blotting after DEX treatment. Determination of activation or repression of *GUS* reporter gene expression by the effector proteins was performed as previously described (Kim et al., 2006). Ten progeny plants from each line were used for GUS activity assays.

Isolation of Mutants

Homozygous *sib1*, *sib2*, and *sig1* mutant plants were identified by PCR using primers corresponding to sequences flanking the T-DNA/transposon insertions (see Supplemental Table 2 online). The *sib1 sib2* double mutants were generated by genetic crossing.

RT-PCR

RT-PCR for detection of *SIB1*, *SIB2*, and *SIG1* transcripts in their respective insertion mutants was performed as previously described (Huang et al., 2010). Total RNA was extracted and treated with DNase to remove contaminating DNA. The treated RNA (1 to 5 mg) was subjected to reverse transcription using the SuperScript III first-strand synthesis system for RT-PCR (Invitrogen). The PCR primers for *SIB1*, *SIB2*, and *SIG1* are listed in Supplemental Table 2 online. The primers used to amplify *ACT2* for PCR were as described previously (Raes et al., 2003; Rohde et al., 2004).

Generation of RNAi-*SIB2* and *RNAI-SIG1* Transgenic Plants

To generate RNAi-*SIB2* transgenic plants, the coding sequence of *SIB2* was amplified with primers (5′-ATCGAGCTCATGGATCAGTCATCAT-CAACGT-3′ and 5′-ATCTCTAGAGAGAGAACCAATGCTTCCTA-3′). The amplified fragment was cloned into a modified RNAi pOCA28 vector at two different sites in reverted orientations (Chen and Chen, 2002). The resulting plasmid was transformed into Columbia-0 (Col-0) wild-type plants and *sib1-2* mutants using the *Agrobacterium*-mediated floral dip procedure (Clough and Bent, 1998). The transformants were identified for resistance to kanamycin.

A *SIG1* DNA fragment was amplified using a pair of primers (5′-ATCGGCGCGCCACTAGTATGGCTACTGCAGCTGTTATAG-3′ and 5′-ATCGGATCCGCACAACTTCCACATGACT-3′). The amplified DNA fragment was inserted into *Asc*I/*Swa*I and *Xba*I/*Bam*HI sites of pFGC5941 in reverse orientations. The generated plasmid was transferred into *Agrobacterium* strain GV3101 and transferred into wild-type plants by floral dip transformation (Clough and Bent, 1998). The transformants were identified for resistance to the BASTA herbicide.

Construction of *SIB1*- and *SIG1*-Overexpressing Transgenic Plants

To generate *SIB1*, *SIB1/VQmut*, and *SIB/NLSmut* overexpression constructs, the coding sequences were amplified using primers 5′-ATCGGCGCGCCGGTCTAGAATGGAGTCATCATCGTCGACT-3′ and 5′-ATCGGATCCCATAGAATCGATGCTTCCAAAG-3′ and their respective DNA fragments as templates. The DNA templates for *SIB1/VQmut* and *SIB/NLSmut* were generated by overlapping PCR as described earlier. To overexpress mutant SIB1 without the N-terminal chloroplast localization signal (*SIB1ΔSP*), a truncated *SIB1* cDNA was first amplified using primers 5′-ATCCCATGGGATTAGACAAGAAAAAACCATCTCC-3′ and 5′-ATTCGCATCCCAAACCCTAT-3′. The amplified *SIB1*, *SIB1/VQmut*, *SIB/NLSmut*, and *SIB1ΔSP* fragments were cloned behind the *CaMV 35S* promoter in the plant transformation vector pOCA30. To generate *SIG1*-overexpressing construct, a full-length cDNA clone for *SIG1* (U16526 from the ABRC at the Ohio State University) was first subcloned into the *Not*I/*Sma*II sites of the pBluescript vector. The resulting plasmid was then digested with *Sac*I/*Sal*I, and the *SIG1* cDNA fragment was placed behind the *CaMV 35S* promoter in a modified pCAMBIA1300P binary vector. Sequences of the overexpression constructs were verified by DNA sequencing. The resulting plasmids were transformed into *Agrobacterium* strain GV3101 and introduced into *Arabidopsis* plants by floral dip transformation (Clough and Bent, 1998). The transformants were screened for resistance to kanamycin (50 μg/mL) or hygromycin (15 μg/mL) as appropriate.

qRT-PCR

Total RNA was extracted with the RNeasy Plant Mini Kit (Qiagen). RNA preparations were treated with DNase using the DNA-free kit from Ambion to remove contaminating DNA, and the treated RNA (1 to 5 μg) was subjected to reverse transcription using the SuperScript III first-strand synthesis system for RT-PCR (Invitrogen). Real-time PCR was conducted using the SYBR PCR Master mix (Applied Biosystems) and run on the ABI Prim 7000 system as previously described (Kim et al., 2008). Quantitative real-time PCR was performed using gene-specific primers: *BcActin* (5′-ATATGTTGGAGATGAAGCGCA-3′ and 5′-ATCATCCCAGTT-GGTGACAA-3′), *Arabidopsis PDF1.2* (5′-CACCCTTATCTTCGCTGCTC-3′ and 5′-GCACAACTTCTGTGCTTCCA-3′), and *UBQ5* (5′-GAAGGCGAAGATC-CAAGACAAG-3′ and 5′-TCCCGGCGAAAATCAATC-3′).

Accession Numbers

Arabidopsis Genome Initiative numbers for the genes discussed in this article are as follows: *WRKY33*, At2g38470; *SIB1*, At3g56710; *SIB2*, At2g41180; *SIG1*, At1g64860; *MKS1*, At3g18690; *MPK4*, At4g01370; *WRKY18*, AT4g31800; WRKY25, AT2g30250; *WRKY48*, At5g49520; *WRKY70*, At3g56400; *PR1*, At2g14610; *PDF1.2*, At5g44420; *ACT2*, AT3G18780; and *UBQ5*, AT3g62250.

Supplemental Data

The following materials are available in the online version of this article.

Supplemental Figure 1. Analysis of SIB1 Protein–Protein Interactions and Subcellular Localization.

Supplemental Figure 2. Bait and Prey Proteins in Yeast Two-Hybrid Assays.

Supplemental Figure 3. Detection of SIB1 in the WRKY33/DNA Complexes.

Supplemental Figure 4. Expression of Effector and *SIB1* Genes for Assaying Transcription-Activating Activity of WRKY33.

Supplemental Figure 5. Structures and Mutants for *SIB1*, *SIB2*, and *SIG1*.

Supplemental Figure 6. Quantitative Real-Time PCR Analysis of *B. cinerea Actin* and *Arabidopsis PDF1.2* Gene Expression.

Supplemental Figure 7. Wild-Type and Mutant *SIB1* Overexpression in Transgenic Plants.

Supplemental Figure 8. *SIG1* Overexpression in Transgenic Plants.

Supplemental Table 1. Primers Used for Generating WRKY33 Deletion Constructs.

Supplemental Table 2. Primers for Mutant Identification and RT-PCR.

ACKNOWLEDGMENTS

We thank the ABRC at the Ohio State University and the Nottingham Arabidopsis Stock Centre for the *Arabidopsis* mutants. This work was supported by the U.S. National Science Foundation (Grant IOS-0958066 to Z.C.) and the National Basic Research Program of China (Grant 2009CB119000 to J.-Q.Y.).

AUTHOR CONTRIBUTIONS

Z.C. and J.-Q.Y. conceived the project. Z.L., Y.L., F.W., Y.C., B.F., and Z.C. designed, performed, and analyzed protein–protein interacting experiments. Z.L., F.W., Y.C., J.-Q.Y., and Z.C. designed, performed, and analyzed mutant and overexpression experiments. Z.L. and Z.C. wrote the article. All authors contributed to the interpretation of data and edited the article.

Received August 16, 2011; revised September 16, 2011; accepted September 29, 2011; published October 11, 2011.

REFERENCES

Andreasson, E., et al. (2005). The MAP kinase substrate MKS1 is a regulator of plant defense responses. EMBO J. **24:** 2579–2589.

Aoyama, T., and Chua, N.-H. (1997). A glucocorticoid-mediated transcriptional induction system in transgenic plants. Plant J. **11:** 605–612.

Benito, E.P., ten Have, A., van't Klooster, J.W., and van Kan, J.A.L. (1998). Fungal and plant gene expression during synchronized infection of tomato leaves by *Botrytis cinerea*. Eur. J. Plant Pathol. **104:** 207–220.

Brodersen, P., Petersen, M., Bjørn Nielsen, H., Zhu, S., Newman, M.A., Shokat, K.M., Rietz, S., Parker, J., and Mundy, J. (2006). Arabidopsis MAP kinase 4 regulates salicylic acid- and jasmonic acid/ethylene-dependent responses via EDS1 and PAD4. Plant J. **47:** 532–546.

Chen, C., and Chen, Z. (2002). Potentiation of developmentally regulated plant defense response by AtWRKY18, a pathogen-induced Arabidopsis transcription factor. Plant Physiol. **129:** 706–716.

Chen, Z., Iyer, S., Caplan, A., Klessig, D.F., and Fan, B. (1997). Differential accumulation of salicylic acid and salicylic acid-sensitive catalase in different rice tissues. Plant Physiol. **114:** 193–201.

Clough, S.J., and Bent, A.F. (1998). Floral dip: A simplified method for Agrobacterium-mediated transformation of *Arabidopsis thaliana*. Plant J. **16:** 735–743.

Cui, X., Fan, B., Scholz, J., and Chen, Z. (2007). Roles of *Arabidopsis* cyclin-dependent kinase C complexes in cauliflower mosaic virus infection, plant growth, and development. Plant Cell **19:** 1388–1402.

de Pater, S., Greco, V., Pham, K., Memelink, J., and Kijne, J. (1996). Characterization of a zinc-dependent transcriptional activator from Arabidopsis. Nucleic Acids Res. **24:** 4624–4631.

Dong, J., Chen, C., and Chen, Z. (2003). Expression profiles of the Arabidopsis WRKY gene superfamily during plant defense response. Plant Mol. Biol. **51:** 21–37.

Ferrari, S., Plotnikova, J.M., De Lorenzo, G., and Ausubel, F.M. (2003). Arabidopsis local resistance to Botrytis cinerea involves salicylic acid and camalexin and requires EDS4 and PAD2, but not SID2, EDS5 or PAD4. Plant J. **35:** 193–205.

Govrin, E.M., and Levine, A. (2000). The hypersensitive response facilitates plant infection by the necrotrophic pathogen *Botrytis cinerea*. Curr. Biol. **10:** 751–757.

Horsfall, J.G., and Dimond, A.E. (1957). Interaction of tissue sugar, growth substance and disease susceptibility. Zeitschr. f. Pflanzenkr. u. Pflanzensch **64:** 415–421.

Huang, J., Gu, M., Lai, Z., Fan, B., Shi, K., Zhou, Y.H., Yu, J.Q., and Chen, Z. (2010). Functional analysis of the Arabidopsis PAL gene family in plant growth, development, and response to environmental stress. Plant Physiol. **153:** 1526–1538.

Ishiguro, S., and Nakamura, K. (1994). Characterization of a cDNA encoding a novel DNA-binding protein, SPF1, that recognizes SP8 sequences in the 5′ upstream regions of genes coding for sporamin and beta-amylase from sweet potato. Mol. Gen. Genet. **244:** 563–571.

Jones, J.D., and Dangl, J.L. (2006). The plant immune system. Nature **444:** 323–329.

Kim, K.C., Fan, B., and Chen, Z. (2006). Pathogen-induced Arabidopsis WRKY7 is a transcriptional repressor and enhances plant susceptibility to *Pseudomonas syringae*. Plant Physiol. **142:** 1180–1192.

Kim, K.C., Lai, Z., Fan, B., and Chen, Z. (2008). Arabidopsis WRKY38 and WRKY62 transcription factors interact with histone deacetylase 19 in basal defense. Plant Cell **20:** 2357–2371.

Lagrimini, L.M., Burkhart, W., Moyer, M., and Rothstein, S. (1987). Molecular cloning of complementary DNA encoding the lignin-forming peroxidase from tobacco: Molecular analysis and tissue-specific expression. Proc. Natl. Acad. Sci. USA **84:** 7542–7546.

Lai, Z., Wang, F., Zheng, Z., Fan, B., and Chen, Z. (2011). A critical role of autophagy in plant resistance to necrotrophic fungal pathogens. Plant J. **66:** 953–968.

Lee, M.W., and Yang, Y. (2006). Transient expression assay by agroinfiltration of leaves. Methods Mol. Biol. **323:** 225–229.

Maleck, K., Levine, A., Eulgem, T., Morgan, A., Schmid, J., Lawton, K.A., Dangl, J.L., and Dietrich, R.A. (2000). The transcriptome of *Arabidopsis thaliana* during systemic acquired resistance. Nat. Genet. **26:** 403–410.

Mao, G., Meng, X., Liu, Y., Zheng, Z., Chen, Z., and Zhang, S. (2011). Phosphorylation of a WRKY transcription factor by two

pathogen-responsive MAPKs drives phytoalexin biosynthesis in Arabidopsis. Plant Cell **23:** 1639–1653.

Mengiste, T., Chen, X., Salmeron, J., and Dietrich, R. (2003b). The BOTRYTIS SUSCEPTIBLE1 gene encodes an R2R3MYB transcription factor protein that is required for biotic and abiotic stress responses in *Arabidopsis*. Plant Cell **15:** 2551–2565.

Mengiste, T., Chen, X., Salmeron, J.M., and Dietrich, R.A. (2003a). The *BOTRYTIS SUSCEPTIBLE1* gene encodes an R2R3MYB transcription factor protein that is required for biotic and abiotic stress responses in *Arabidopsis*. Plant Cell **15:** 2551–2565.

Moor, W.D. (1942). Some factors affecting the infection of tomato seedlings by *Alternaria solani*. Phytopathology **32:** 399–403.

Moor, W.D., and Thomas, H.R. (1943). Some cultural practices that influence the development of *Alternaria solani* on tomato seedlings. Phytopathology **33:** 1176–1184.

Morikawa, K., Shiina, T., Murakami, S., and Toyoshima, Y. (2002). Novel nuclear-encoded proteins interacting with a plastid sigma factor, Sig1, in *Arabidopsis thaliana*. FEBS Lett. **514:** 300–304.

Nandi, A., Moeder, W., Kachroo, P., Klessig, D.F., and Shah, J. (2005). Arabidopsis ssi2-conferred susceptibility to *Botrytis cinerea* is dependent on EDS5 and PAD4. Mol. Plant Microbe Interact. **18:** 363–370.

Narusaka, M., Kawai, K., Izawa, N., Seki, M., Shinozaki, K., Seo, S., Kobayashi, M., Shiraishi, T., and Narusaka, Y. (2008). Gene coding for SigA-binding protein from Arabidopsis appears to betranscriptionally up-regulated by salicylic acid and NPR1-dependent mechanism. J. Gen. Plant Pathol. **74:** 345–354.

Penninckx, I.A., Eggermont, K., Terras, F.R., Thomma, B.P., De Samblanx, G.W., Buchala, A., Métraux, J.P., Manners, J.M., and Broekaert, W.F. (1996). Pathogen-induced systemic activation of a plant defensin gene in *Arabidopsis* follows a salicylic acid-independent pathway. Plant Cell **8:** 2309–2323.

Penninckx, I.A., Thomma, B.P., Buchala, A., Métraux, J.P., and Broekaert, W.F. (1998). Concomitant activation of jasmonate and ethylene response pathways is required for induction of a plant defensin gene in *Arabidopsis*. Plant Cell **10:** 2103–2113.

Perruc, E., Charpenteau, M., Ramirez, B.C., Jauneau, A., Galaud, J.P., Ranjeva, R., and Ranty, B. (2004). A novel calmodulin-binding protein functions as a negative regulator of osmotic stress tolerance in *Arabidopsis thaliana* seedlings. Plant J. **38:** 410–420.

Petersen, K., Qiu, J.L., Lütje, J., Fiil, B.K., Hansen, S., Mundy, J., and Petersen, M. (2010). Arabidopsis MKS1 is involved in basal immunity and requires an intact N-terminal domain for proper function. PLoS ONE **5:** e14364.

Qiu, J.L., et al. (2008). Arabidopsis MAP kinase 4 regulates gene expression through transcription factor release in the nucleus. EMBO J. **27:** 2214–2221.

Raes, J., Rohde, A., Christensen, J.H., Van de Peer, Y., and Boerjan, W. (2003). Genome-wide characterization of the lignification toolbox in Arabidopsis. Plant Physiol. **133:** 1051–1071.

Rohde, A., et al. (2004). Molecular phenotyping of the pal1 and pal2 mutants of *Arabidopsis thaliana* reveals far-reaching consequences on phenylpropanoid, amino acid, and carbohydrate metabolism. Plant Cell **16:** 2749–2771.

Rowell, J.B. (1953). Leaf blight of tomato and potato plants-factors affecting the degree of injury incted by *Alternaria solani*. R. I. Agric. Exp. Stat. Bull. **320:** 290.

Rushton, P.J., Somssich, I.E., Ringler, P., and Shen, Q.J. (2010). WRKY transcription factors. Trends Plant Sci. **15:** 247–258.

Shimizu, M., Kato, H., Ogawa, T., Kurachi, A., Nakagawa, Y., and Kobayashi, H. (2010). Sigma factor phosphorylation in the photosynthetic control of photosystem stoichiometry. Proc. Natl. Acad. Sci. USA **107:** 10760–10764.

Thomma, B.P., Eggermont, K., Penninckx, I.A., Mauch-Mani, B., Vogelsang, R., Cammue, B.P.A., and Broekaert, W.F. (1998). Separate jasmonate-dependent and salicylate-dependent defense-response pathways in Arabidopsis are essential for resistance to distinct microbial pathogens. Proc. Natl. Acad. Sci. USA **95:** 15107–15111.

Thomma, B.P., Nelissen, I., Eggermont, K., and Broekaert, W.F. (1999). Deficiency in phytoalexin production causes enhanced susceptibility of *Arabidopsis thaliana* to the fungus *Alternaria brassicicola*. Plant J. **19:** 163–171.

Turck, F., Zhou, A., and Somssich, I.E. (2004). Stimulus-dependent, promoter-specific binding of transcription factor WRKY1 to its native promoter and the defense-related gene PcPR1-1 in parsley. Plant Cell **16:** 2573–2585.

Veronese, P., Chen, X., Bluhm, B., Salmeron, J., Dietrich, R.A., and Mengiste, T. (2004). The BOS loci of Arabidopsis are required for resistance to *Botrytis cinerea* infection. Plant J. **40:** 558–574.

Veronese, P., Nakagami, H., Bluhm, B., Abuqamar, S., Chen, X., Salmeron, J., Dietrich, R.A., Hirt, H., and Mengiste, T. (2006). The membrane-anchored BOTRYTIS-INDUCED KINASE1 plays distinct roles in *Arabidopsis* resistance to necrotrophic and biotrophic pathogens. Plant Cell **18:** 257–273.

Wang, A., Garcia, D., Zhang, H., Feng, K., Chaudhury, A., Berger, F., Peacock, W.J., Dennis, E.S., and Luo, M. (2010). The VQ motif protein IKU1 regulates endosperm growth and seed size in Arabidopsis. Plant J. **63:** 670–679.

Xie, Y.D., Li, W., Guo, D., Dong, J., Zhang, Q., Fu, Y., Ren, D., Peng, M., and Xia, Y. (2010). The Arabidopsis gene SIGMA FACTOR-BINDING PROTEIN 1 plays a role in the salicylate- and jasmonate-mediated defence responses. Plant Cell Environ. **33:** 828–839.

Xing, D., and Chen, Z. (2006). Effects of mutations and constitutive overexpression of EDS1 and PAD4 on plant resistance to different types of microbial pathogens. Plant Sci. **171:** 251–262.

Xing, D.H., Lai, Z.B., Zheng, Z.Y., Vinod, K.M., Fan, B.F., and Chen, Z.X. (2008). Stress- and pathogen-induced Arabidopsis WRKY48 is a transcriptional activator that represses plant basal defense. Mol. Plant **1:** 459–470.

Xu, X., Chen, C., Fan, B., and Chen, Z. (2006). Physical and functional interactions between pathogen-induced *Arabidopsis* WRKY18, WRKY40, and WRKY60 transcription factors. Plant Cell **18:** 1310–1326.

Zhang, Y., and Wang, L. (2005). The WRKY transcription factor superfamily: Its origin in eukaryotes and expansion in plants. BMC Evol. Biol. **5:** 1.

Zheng, Z., Qamar, S.A., Chen, Z., and Mengiste, T. (2006). Arabidopsis WRKY33 transcription factor is required for resistance to necrotrophic fungal pathogens. Plant J. **48:** 592–605.